International Journal of Physical Sciences

Volume 8 Number 27 23 July, 2013

ISSN 1992-1950

Academic Journals

ABOUT IJPS

The **International Journal of Physical Sciences (IJPS)** is published weekly (one volume per year) by Academic Journals.

International Journal of Physical Sciences (IJPS) is an open access journal that publishes high-quality solicited and unsolicited articles, in English, in all Physics and chemistry including artificial intelligence, neural processing, nuclear and particle physics, geophysics, physics in medicine and biology, plasma physics, semiconductor science and technology, wireless and optical communications, materials science, energy and fuels, environmental science and technology, combinatorial chemistry, natural products, molecular therapeutics, geochemistry, cement and concrete research, metallurgy, crystallography and computer-aided materials design. All articles published in IJPS are peer-reviewed.

Submission of Manuscript

Submit manuscripts as e-mail attachment to the Editorial Office at: ijps@academicjournals.org. A manuscript number will be mailed to the corresponding author shortly after submission.

For all other correspondence that cannot be sent by e-mail, please contact the editorial office (at ijps@academicjournals.org).

The International Journal of Physical Sciences will only accept manuscripts submitted as e-mail attachments.

Please read the **Instructions for Authors** before submitting your manuscript. The manuscript files should be given the last name of the first author.

Editors

Prof. Sanjay Misra
Department of Computer Engineering, School of Information and Communication Technology
Federal University of Technology, Minna,
Nigeria.

Prof. Songjun Li
School of Materials Science and Engineering,
Jiangsu University,
Zhenjiang,
China

Dr. G. Suresh Kumar
Senior Scientist and Head Biophysical Chemistry
Division Indian Institute of Chemical Biology
(IICB)(CSIR, Govt. of India),
Kolkata 700 032,
INDIA.

Dr. 'Remi Adewumi Oluyinka
Senior Lecturer,
School of Computer Science
Westville Campus
University of KwaZulu-Natal
Private Bag X54001
Durban 4000
South Africa.

Prof. Hyo Choi
Graduate School
Gangneung-Wonju National University
Gangneung,
Gangwondo 210-702, Korea

Prof. Kui Yu Zhang
Laboratoire de Microscopies et d'Etude de Nanostructures (LMEN)
Département de Physique, Université de Reims,
B.P. 1039. 51687,
Reims cedex,
France.

Prof. R. Vittal
Research Professor,
Department of Chemistry and Molecular Engineering
Korea University, Seoul 136-701,
Korea.

Prof Mohamed Bououdina
Director of the Nanotechnology Centre
University of Bahrain
PO Box 32038,
Kingdom of Bahrain

Prof. Geoffrey Mitchell
School of Mathematics,
Meteorology and Physics
Centre for Advanced Microscopy
University of Reading Whiteknights,
Reading RG6 6AF
United Kingdom.

Prof. Xiao-Li Yang
School of Civil Engineering,
Central South University,
Hunan 410075,
China

Dr. Sushil Kumar
Geophysics Group,
Wadia Institute of Himalayan Geology,
P.B. No. 74 Dehra Dun - 248001(UC)
India.

Prof. Suleyman KORKUT
Duzce University
Faculty of Forestry
Department of Forest Industrial Engineeering
Beciyorukler Campus 81620
Duzce-Turkey

Prof. Nazmul Islam
Department of Basic Sciences & Humanities/Chemistry,
Techno Global-Balurghat, Mangalpur, Near District Jail P.O: Beltalapark, P.S: Balurghat, Dist.: South Dinajpur,
Pin: 733103,India.

Prof. Dr. Ismail Musirin
Centre for Electrical Power Engineering Studies (CEPES), Faculty of Electrical Engineering, Universiti Teknologi Mara,
40450 Shah Alam,
Selangor, Malaysia

Prof. Mohamed A. Amr
Nuclear Physic Department, Atomic Energy Authority
Cairo 13759,
Egypt.

Dr. Armin Shams
Artificial Intelligence Group,
Computer Science Department,
The University of Manchester.

Editorial Board

Prof. Salah M. El-Sayed
Mathematics. Department of Scientific Computing.
Faculty of Computers and Informatics,
Benha University. Benha ,
Egypt.

Dr. Rowdra Ghatak
Associate Professor
Electronics and Communication Engineering Dept.,
National Institute of Technology Durgapur
Durgapur West Bengal

Prof. Fong-Gong Wu
College of Planning and Design, National Cheng Kung University
Taiwan

Dr. Abha Mishra.
Senior Research Specialist & Affiliated Faculty.
Thailand

Dr. Madad Khan
Head
Department of Mathematics
COMSATS University of Science and Technology
Abbottabad, Pakistan

Prof. Yuan-Shyi Peter Chiu
Department of Industrial Engineering & Management
Chaoyang University of Technology
Taichung, Taiwan

Dr. M. R. Pahlavani,
Head, Department of Nuclear physics,
Mazandaran University,
Babolsar-Iran

Dr. Subir Das,
Department of Applied Mathematics,
Institute of Technology, Banaras Hindu University,
Varanasi

Dr. Anna Oleksy
Department of Chemistry
University of Gothenburg
Gothenburg,
Sweden

Prof. Gin-Rong Liu,
Center for Space and Remote Sensing Research
National Central University, Chung-Li,
Taiwan 32001

Prof. Mohammed H. T. Qari
Department of Structural geology and remote sensing
Faculty of Earth Sciences
King Abdulaziz UniversityJeddah,
Saudi Arabia

Dr. Jyhwen Wang,
Department of Engineering Technology and Industrial Distribution
Department of Mechanical Engineering
Texas A&M University
College Station,

Prof. N. V. Sastry
Department of Chemistry
Sardar Patel University
Vallabh Vidyanagar
Gujarat, India

Dr. Edilson Ferneda
Graduate Program on Knowledge Management and IT,
Catholic University of Brasilia,
Brazil

Dr. F. H. Chang
Department of Leisure, Recreation and Tourism Management,
Tzu Hui Institute of Technology, Pingtung 926,
Taiwan (R.O.C.)

Prof. Annapurna P.Patil,
Department of Computer Science and Engineering,
M.S. Ramaiah Institute of Technology, Bangalore-54,
India.

Dr. Ricardo Martinho
Department of Informatics Engineering, School of Technology and Management, Polytechnic Institute of Leiria, Rua General Norton de Matos, Apartado 4133, 2411-901 Leiria,
Portugal.

Dr Driss Miloud
University of mascara / Algeria
Laboratory of Sciences and Technology of Water
Faculty of Sciences and the Technology
Department of Science and Technology
Algeria

Instructions for Author

Electronic submission of manuscripts is strongly encouraged, provided that the text, tables, and figures are included in a single Microsoft Word file (preferably in Arial font).

The **cover letter** should include the corresponding author's full address and telephone/fax numbers and should be in an e-mail message sent to the Editor, with the file, whose name should begin with the first author's surname, as an attachment.

Article Types

Three types of manuscripts may be submitted:

Regular articles: These should describe new and carefully confirmed findings, and experimental procedures should be given in sufficient detail for others to verify the work. The length of a full paper should be the minimum required to describe and interpret the work clearly.

Short Communications: A Short Communication is suitable for recording the results of complete small investigations or giving details of new models or hypotheses, innovative methods, techniques or apparatus. The style of main sections need not conform to that of full-length papers. Short communications are 2 to 4 printed pages (about 6 to 12 manuscript pages) in length.

Reviews: Submissions of reviews and perspectives covering topics of current interest are welcome and encouraged. Reviews should be concise and no longer than 4-6 printed pages (about 12 to 18 manuscript pages). Reviews are also peer-reviewed.

Review Process

All manuscripts are reviewed by an editor and members of the Editorial Board or qualified outside reviewers. Authors cannot nominate reviewers. Only reviewers randomly selected from our database with specialization in the subject area will be contacted to evaluate the manuscripts. The process will be blind review.

Decisions will be made as rapidly as possible, and the journal strives to return reviewers' comments to authors as fast as possible. The editorial board will re-review manuscripts that are accepted pending revision. It is the goal of the IJPS to publish manuscripts within weeks after submission.

Regular articles

All portions of the manuscript must be typed double-spaced and all pages numbered starting from the title page.

The Title should be a brief phrase describing the contents of the paper. The Title Page should include the authors' full names and affiliations, the name of the corresponding author along with phone, fax and E-mail information. Present addresses of authors should appear as a footnote.

The Abstract should be informative and completely self-explanatory, briefly present the topic, state the scope of the experiments, indicate significant data, and point out major findings and conclusions. The Abstract should be 100 to 200 words in length.. Complete sentences, active verbs, and the third person should be used, and the abstract should be written in the past tense. Standard nomenclature should be used and abbreviations should be avoided. No literature should be cited.

Following the abstract, about 3 to 10 key words that will provide indexing references should be listed.

A list of non-standard **Abbreviations** should be added. In general, non-standard abbreviations should be used only when the full term is very long and used often. Each abbreviation should be spelled out and introduced in parentheses the first time it is used in the text. Only recommended SI units should be used. Authors should use the solidus presentation (mg/ml). Standard abbreviations (such as ATP and DNA) need not be defined.

The Introduction should provide a clear statement of the problem, the relevant literature on the subject, and the proposed approach or solution. It should be understandable to colleagues from a broad range of scientific disciplines.

Materials and methods should be complete enough to allow experiments to be reproduced. However, only truly new procedures should be described in detail; previously published procedures should be cited, and important modifications of published procedures should be mentioned briefly. Capitalize trade names and include the manufacturer's name and address. Subheadings should be used. Methods in general use need not be described in detail.

Results should be presented with clarity and precision. The results should be written in the past tense when describing findings in the authors' experiments. Previously published findings should be written in the present tense. Results should be explained, but largely without referring to the literature. Discussion, speculation and detailed interpretation of data should not be included in the Results but should be put into the Discussion section.

The Discussion should interpret the findings in view of the results obtained in this and in past studies on this topic. State the conclusions in a few sentences at the end of the paper. The Results and Discussion sections can include subheadings, and when appropriate, both sections can be combined.

The Acknowledgments of people, grants, funds, etc should be brief.

Tables should be kept to a minimum and be designed to be as simple as possible. Tables are to be typed double-spaced throughout, including headings and footnotes. Each table should be on a separate page, numbered consecutively in Arabic numerals and supplied with a heading and a legend. Tables should be self-explanatory without reference to the text. The details of the methods used in the experiments should preferably be described in the legend instead of in the text. The same data should not be presented in both table and graph form or repeated in the text.

Figure legends should be typed in numerical order on a separate sheet. Graphics should be prepared using applications capable of generating high resolution GIF, TIFF, JPEG or Powerpoint before pasting in the Microsoft Word manuscript file. Tables should be prepared in Microsoft Word. Use Arabic numerals to designate figures and upper case letters for their parts (Figure 1). Begin each legend with a title and include sufficient description so that the figure is understandable without reading the text of the manuscript. Information given in legends should not be repeated in the text.

References: In the text, a reference identified by means of an author‘s name should be followed by the date of the reference in parentheses. When there are more than two authors, only the first author‘s name should be mentioned, followed by ’et al‘. In the event that an author cited has had two or more works published during the same year, the reference, both in the text and in the reference list, should be identified by a lower case letter like ’a‘ and ’b‘ after the date to distinguish the works.

Examples:

Abayomi (2000), Agindotan et al. (2003), (Kelebeni, 1983), (Usman and Smith, 1992), (Chege, 1998; 1987a,b; Tijani, 1993,1995), (Kumasi et al., 2001)

References should be listed at the end of the paper in alphabetical order. Articles in preparation or articles submitted for publication, unpublished observations, personal communications, etc. should not be included in the reference list but should only be mentioned in the article text (e.g., A. Kingori, University of Nairobi, Kenya, personal communication). Journal names are abbreviated according to Chemical Abstracts. Authors are fully responsible for the accuracy of the references.

Examples:

Ogunseitan OA (1998). Protein method for investigating mercuric reductase gene expression in aquatic environments. Appl. Environ. Microbiol. 64:695-702.

Gueye M, Ndoye I, Dianda M, Danso SKA, Dreyfus B (1997). Active N2 fixation in several Faidherbia albida provenances. Ar. Soil Res. Rehabil. 11:63-70.

Charnley AK (1992). Mechanisms of fungal pathogenesis in insects with particular reference to locusts. In: Lomer CJ, Prior C (eds) Biological Controls of Locusts and Grasshoppers: Proceedings of an international workshop held at Cotonou, Benin. Oxford: CAB International, pp 181-190.

Mundree SG, Farrant JM (2000). Some physiological and molecular insights into the mechanisms of desiccation tolerance in the resurrection plant Xerophyta viscasa Baker. In Cherry et al. (eds) Plant tolerance to abiotic stresses in Agriculture: Role of Genetic Engineering, Kluwer Academic Publishers, Netherlands, pp 201-222.

Short Communications

Short Communications are limited to a maximum of two figures and one table. They should present a complete study that is more limited in scope than is found in full-length papers. The items of manuscript preparation listed above apply to Short Communications with the following differences: (1) Abstracts are limited to 100 words; (2) instead of a separate Materials and Methods section, experimental procedures may be incorporated into Figure Legends and Table footnotes; (3) Results and Discussion should be combined into a single section.

Proofs and Reprints: Electronic proofs will be sent (e-mail attachment) to the corresponding author as a PDF file. Page proofs are considered to be the final version of the manuscript. With the exception of typographical or minor clerical errors, no changes will be made in the manuscript at the proof stage.

Copyright: © 2013, Academic Journals.
All rights Reserved. In accessing this journal, you agree that you will access the contents for your own personal use but not for any commercial use. Any use and or copies of this Journal in whole or in part must include the customary bibliographic citation, including author attribution, date and article title.

Submission of a manuscript implies: that the work described has not been published before (except in the form of an abstract or as part of a published lecture, or thesis) that it is not under consideration for publication elsewhere; that if and when the manuscript is accepted for publication, the authors agree to automatic transfer of the copyright to the publisher.

Disclaimer of Warranties

In no event shall Academic Journals be liable for any special, incidental, indirect, or consequential damages of any kind arising out of or in connection with the use of the articles or other material derived from the IJPS, whether or not advised of the possibility of damage, and on any theory of liability.
This publication is provided "as is" without warranty of any kind, either expressed or implied, including, but not limited to, the implied warranties of merchantability, fitness for a particular purpose, or non-infringement. Descriptions of, or references to, products or publications does not imply endorsement of that product or publication. While every effort is made by Academic Journals to see that no inaccurate or misleading data, opinion or statements appear in this publication, they wish to make it clear that the data and opinions appearing in the articles and advertisements herein are the responsibility of the contributor or advertiser concerned. Academic Journals makes no warranty of any kind, either express or implied, regarding the quality, accuracy, availability, or validity of the data or information in this publication or of any other publication to which it may be linked.

International Journal of Physical Sciences

Table of Contents: Volume 8 Number 27 23 July, 2013

ARTICLES

APPLIED SCIENCE

ENVIRONMENTAL AND EARTH SCIENCES

academicJournals

Vol. 8(27), pp. 1408-1416, 23 July, 2013
DOI: 10.5897/IJPS2013.3948
ISSN 1992 - 1950 © 2013 Academic Journals
http://www.academicjournals.org/IJPS

International Journal of Physical Sciences

Full Length Research Paper

Anti-islanding protection based on voltage and frequency analysis in wind turbines units

Behrooz Sobhani* and Noradin Ghadimi

Department of Electrical Engineering, Ardabil Branch, Islamic Azad University, Ardabil, Iran.

Accepted 19 July, 2013

This paper introduces a new islanding detection algorithm method based on voltage and frequency analysis for wind turbines as distributed resource units at the distribution voltage level. The proposed method is based on processing of the rate of change of q-axis component of voltage and accelerates of change of frequency. This method detects the islanding conditions with the analysis of these signals. The studies reported in this paper are based on time-domain simulations using MATLAB, and the feasibility of the proposed method is evaluated with an experimental system. The experimental system parameters are the same as those of the simulated system. The results show that the proposed islanding detection method succeeds in detecting islanding both in the experimental and simulated systems.

Key words: Islanding protection, wind turbine simulator, distributed generation, accelerates of change of frequency (ACOF)-ROCOQA- dq-component.

INTRODUCTION

The increase of distributed resources in the electric utility systems is indicated due to recent and ongoing technological, social, economical and environmental aspects. Distributed generation (DG) units have become more competitive against the conventional centralized system by successfully integrating new generation technologies and power electronics. Hence, it attracts many customers from industrial, commercial, and residential sectors. DGs generally refer to distributed energy resources (DERs), including photovoltaic, fuel cells, micro turbines, and small wind turbines, and additional equipment (Jiayi et al., 2008).

The total global installed wind capacity at the end of 2010 was 430 TWh annually, which is 2.5% of the total global demand. Based on the current growth rates, World Wide Energy Association (WWEA) predicts that, in 2015, a global capacity of 600 GW is possible. By the end of the year 2020, at least 1500 GW can be expected to be installed globally (http://www.renewableenergyworld.com/rea/news/article/2011/05/worldwind-outlook- down-but-not-out). However, connecting wind turbines to distribution networks produces some problems, such as islanding.

Islanding occurs when a DG and its local load become electrically isolated from the utility; meanwhile, the DG produces electrical energy and supplies the local load (Jayaweera et al., 2007) Islanding creates many problems in power systems, and the existing standards thus do not permit DGs to be utilized in islanding mode (Zeineldin et al., 2007). Some of these reasons are the following (Wilsun et al., 2004; Swisher et al., 2001).

(i) Safety hazards for personnel
(ii) Power quality problems for customers load
(iii) Overload conditions of DG
(iv) Out-of-phase recloser connections

*Corresponding author. E-mail: b.sobhani@gmail.com.

Thus, islanding conditions should be detected within less than 2 s (Wilsun et al., 2004). Originally, the methods of islanding detection were divided into two categories: communication and local. Local methods were classified as active and passive techniques, in which active techniques are based on direct interaction with the ongoing power system operation (Zeineldin et al., 2007). Some important active techniques are impedance measurement (Chowdhury et al., 2009) frequency shift and active frequency drift (Chowdhury et al., 2009), current injection (Guillermo and Reza, 2006), sandia frequency shift and sandia voltage shift (Vinod et al., 2004), and negative phase sequence current injection (Karimi et al., 2008). Passive techniques are based on measurements and information at the local site. Some techniques are under/over frequency or voltage (Chowdhury et al., 2009), total harmonic distortions (http://www.renewableenergyworld.com/rea/news/article/2011/05/worldwind-outlook-down-but-not-out), rate of change of frequency (ROCOF) (El-Arroudi et al., 2007), vector surge and phase displacement monitoring (Kunte and Gao, 2008), rate of change of generator power output (Chowdhury et al., 2009), and the THD technique (Kazemi and Shataee, 2008).

In this paper, a new technique based on rate of change of q-axes component of voltage (ROCOQAC) and accelerate of change of frequency (ACOF) is proposed for islanding detection of wind turbines. The simulation test systems were simulated in MATLAB/SIMULINK using Sim Power System Block Set. The simulation and experimental results show that the proposed islanding detection technique works well to discriminate between switching and islanding conditions.

Proposed technique

ROCOQAC algorithm uses synchronous transformation based phasor estimation of the retrieved instantaneous voltage signals. The signal *x(t)* is represented as follows:

$$X(t) = \sum_{n=1}^{\infty} X_{\max} \cos(n\omega_0 t + \phi_n) \quad (1)$$

Under balanced conditions, each three-phase variable $x_{abc}(t)$ of Equation (1) can be transferred to a stationary $\alpha\beta$ reference frame system by applying the following abc to $\alpha\beta$ transformation:

$$x_{\alpha\beta} = x_a e^{j0} + x_b e^{j2\pi/3} + x_c e^{-j2\pi/3} \quad (2)$$

Where $x_{\alpha\beta} = x_\alpha + jx_\beta$, in order to calculating dq parameters can be used of Equation (3):

$$x_d + jx_q = x_{\alpha\beta} e^{-j\theta} \quad (3)$$

where θ calculated by:

$$\theta = \arctan\frac{x_\beta^{ref}}{x_\alpha^{ref}} \quad (4)$$

One of the excising algorithms for detection of islanding is based on accelerates of change of frequency (ACOF). In this method, Frequency of DG unit is regularly measured and accelerates of change of Frequency is calculated the ACOF, is calculated as:

$$ROCOF = \frac{d^2 f}{dt^2} \quad (5)$$

Islanding condition can be detected by comparison of value of ACOF with a threshold. However, this method is not reliable. Islanding and some other events, such as switching of motors and capacitor banks, may have similar effect on *ACOF*, thus the algorithm may take incorrect decision and interrupt the production of DG in a wrong way.

Here, we propose a new algorithm that employs both ACOF and ROCOQAC in order to detect the islanding event. Figure 1 shows algorithm of the proposed method. In the first step, the frequency of load voltage is measured for ten cycles (0.2 s); ACOF is calculated afterwards. The accelerate of change of frequency is calculated by Equation (5). In next step, ACOF has been compared with its threshold values. If the value of ACOF in some portions of the measurement period (0.2 s) exceeds the threshold value then, ROCOQAC will be calculated and if its value exceeds from its threshold too, in this case islanding will be detected. In other cases when one of them doesn't exceed from their threshold, system will be continue to power production (Figure 1). In this study the threshold value of ACOF set to 75 mHZ/S2 and ROCOQAC threshold value set to 250 V/sec.

Case study

Figure 2 shows a schematic diagram of a wind turbine unit. The DG unit is a wind turbine induction generator, and a capacitor bank is used to improve the power factor. The local load is a three-phase parallel RL before the circuit breaker (CB), in which "r" denotes the series resistance inductance and V_f indicates the voltage drop across the parallel load. The parallel RL is conventionally adopted as the local load for the evaluation of islanding detection methods when the load inductance is tuned to the system frequency. This system, as shown in Figure 2, is connected to a point of common coupling (PCC) with a step-up transformer. To obtain the experimental results, a wind turbine simulator, as shown in Figure 3, was implemented. Figure 4 shows the implemented simulator system. The implemented system parameters are given in Table 1. The parallel load inductance is considered infinite. Thus, the parallel load is only a resistance, and hence the unit of "L" is "inf". Figure 5 shows the motor saturation curve. In the grid-connected condition, the switches SW1 and SW2 are closed. The islanding condition occurs when SW2 is open. The voltage and frequency of DG should have admissible values in both grid-connected and islanded modes. In the grid-connected mode, the voltage magnitude and frequency of the local load at the PCC are regulated by the grid.

Implementation and simulation results

In this study, the simulation is conducted in four scenarios to illustrate the effectiveness of the proposed method.

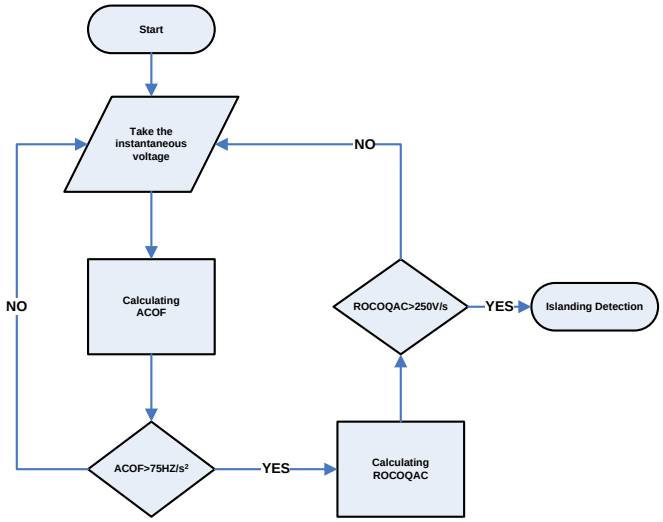

Figure 1. Proposed algorithm in order to islanding detection.

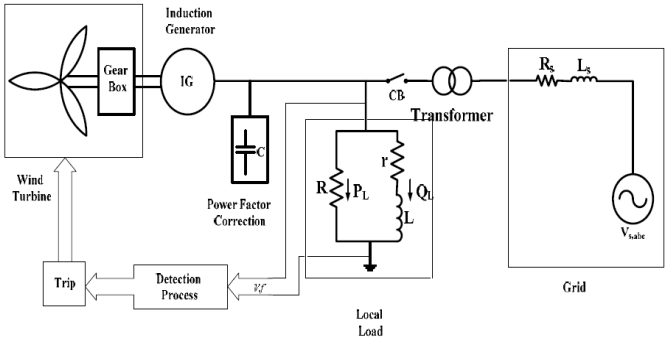

Figur 2. Single line diagram of study system.

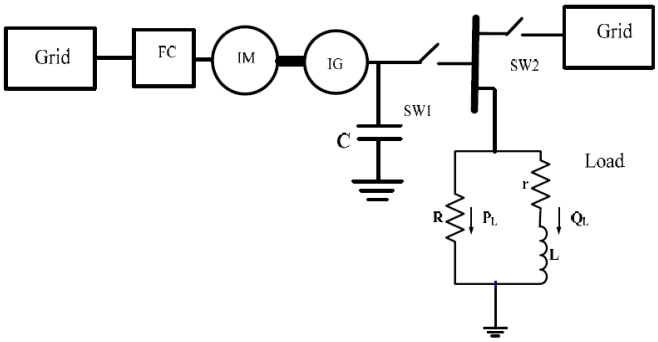

Figure 3. Single line diagram of implementation system in order to islanding condition detection.

Load condition 1

In this case, the load as shown in Figure 2 is set to the values given in Table 1. The DG is connected to the grid and works in grid-connected mode. At t=2 s, the CB is opened, and the system enters islanding mode. Figure 6 shows the dynamic response of the system prior, during and subsequent to the islanding event. Figure 6(a) and

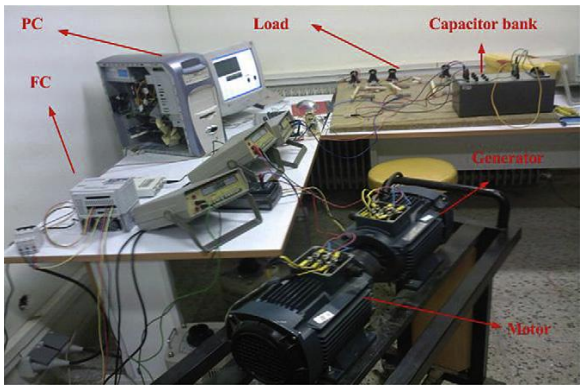

Figure 4. Implementation system in order to islanding condition detection.

Table 1. Parameters of the implemented system.

Parameter		Value
Induction motors	Sn	2KVA
	Vn	400V
	f	50HZ
	PF	0.78Lag
	Rs, Rr	2.3541Ω
	Lr, Ls	0.01678H
	Lm	0.275H
Local load	R	180Ω
	L	Inf
Capacitor	C	36.75 µF

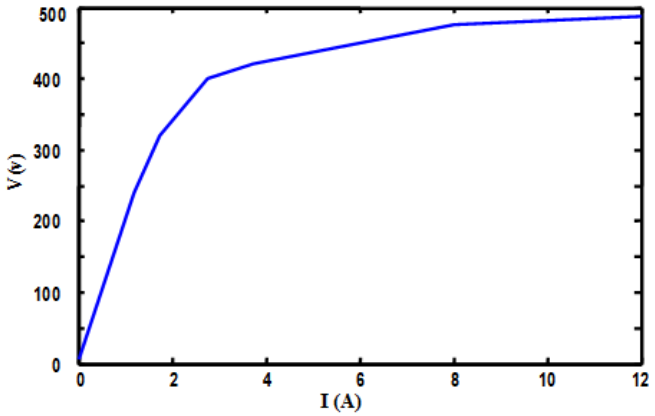

Figure 5. Motor and generator saturation curves.

(b) shows the Δf and voltage of the load and demonstrates that they have no main change prior to the islanding and after the islanding condition. Figure 6(c) shows the ACOF and Figure 6(d) depict the ROCOQAC. According to these figures, at t=2.18 s, the ACOF increases from threshold value. And at t=2.03 s the

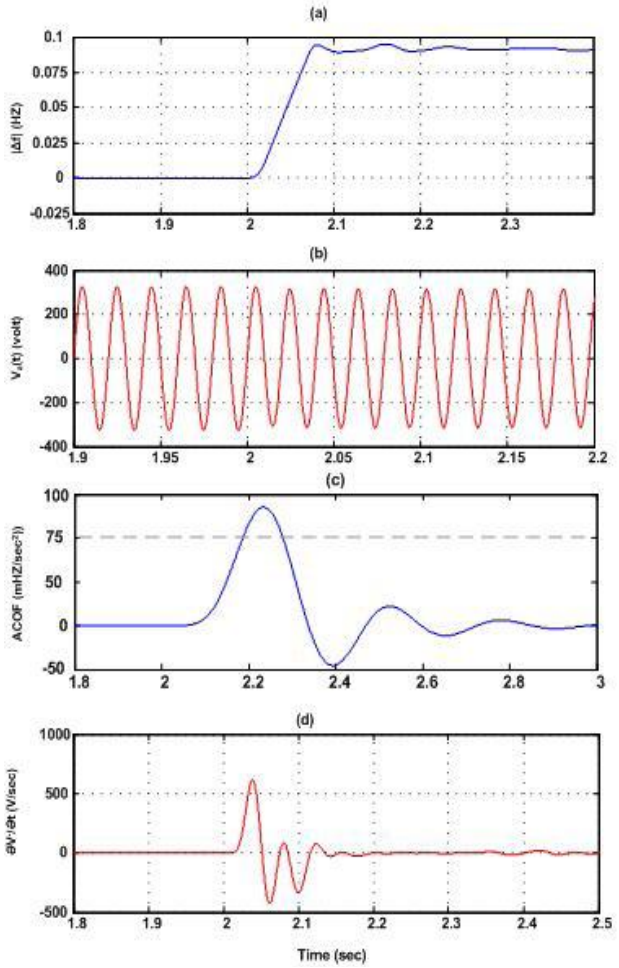

Figure 6. Dynamic response of the simulation system in load condition 1, a) frequency of PCC, b) Instantaneous voltage of phase-a , c) accelerate of change of frequency, d) rate of change of q-component of voltage.

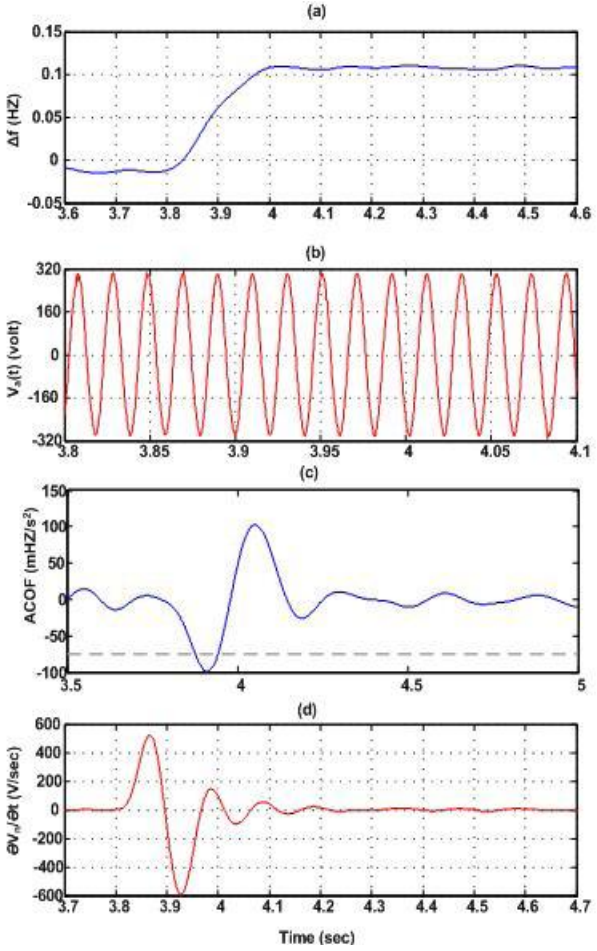

Figure 7. Dynamic response of the experimental system in load condition 1, a) frequency of PCC, b) Instantaneous voltage of phase-a , c) accelerate of change of frequency, d) rate of change of q-component of voltage.

ROCOQAC increases from threshold too. Therefore, the proposed method detects the islanding. In Figure 7, the experimental results for the nominal load are depicted. In the experimental case islanding occurred at t=3.75s. Figure 7(a) shows the Δf of the load and demonstrates that is almost fixed prior to the islanding. Figure 7(b) depicted the instantaneous voltage of phase-a at the PCC. According to these figure the voltage of utility is fixed before islanding, and after islanding. Figure 7(c) and (d) shows the ACOF and ROCOQAC respectively. As shown, the ACOF is increased from the threshold value at t = 3.88s and ROCOQAC increased from the threshold value at t = 3.84s, which leads to islanding detection.

Load condition 2

The system shown in Figure 2 operates in a grid-connected mode. The load absorbs 200 W of real power from the grid and sends 140 var reactive power to the grid and 600 W real powers from the DG. The load parameters are R = 180.5 Ω, L = 3H and C = 40 mF. An islanding event occurs at t=2 s and is detected at t=2.175 s with the ACOF and ROCOQAC (Figure 8c and d). The islanding detection time is shorter than in the previous case study. The voltage magnitude at the PCC and the islanded system frequency change rapidly, but these values do not deviate from their acceptable limits. Figure 8 shows the results of this condition in the simulated system. According to Figure 8(b), the value of the voltage is decreased after islanding, and the frequency of the system, as shown in Figure 8(a), is increased.

The results for the experimental system are depicted in Figure 9. Figure 9(a) and (b) illustrate the Δf and voltage of the load respectively. The voltage of utility is decreased after islanding. Figure 9(c) and (d) shows the ACOF and ROCOQAC values respectively. In this case, at t = 1.2 s, islanding occurs and is detected at t = 1.37 s.

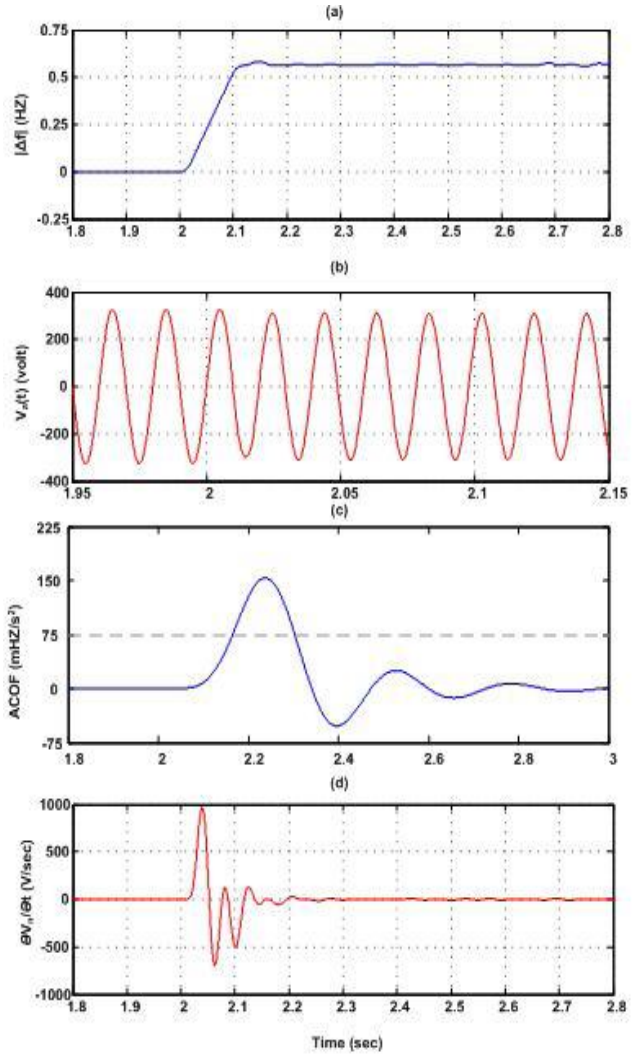

Figure 8. Dynamic response of the simulation system in load condition 2, a) frequency of PCC, b) Instantaneous voltage of phase-a , c) accelerate of change of frequency, d) rate of change of q-component of voltage.

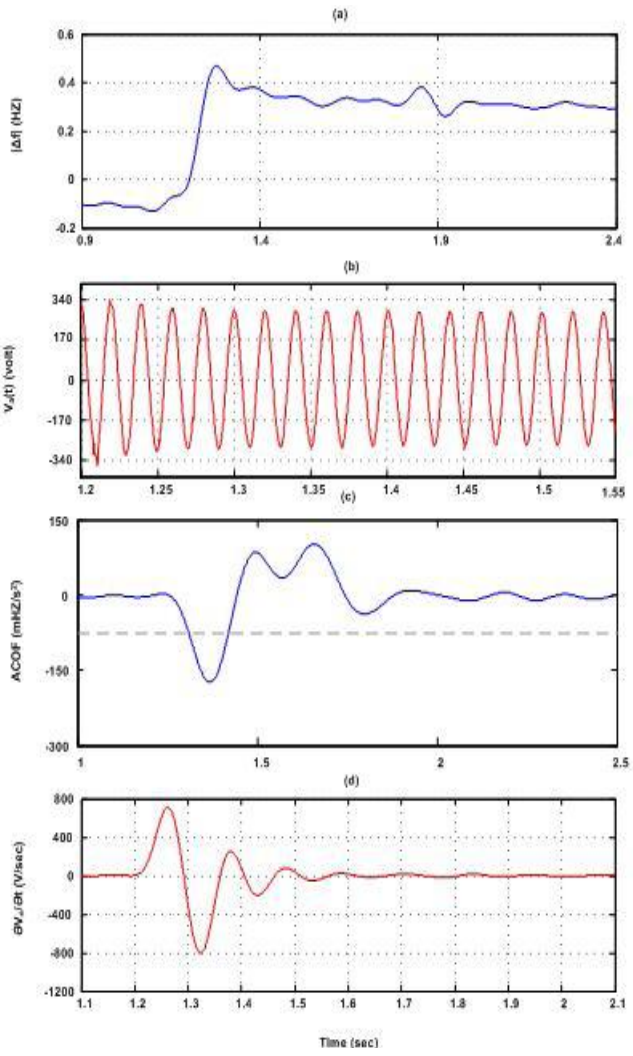

Figure 9. Dynamic response of the experimental system in load condition 2, a) frequency of PCC, b) Instantaneous voltage of phase-a , c) accelerate of change of frequency, d) rate of change of q-component of voltage.

Motor starting condition

The starting of large induction motors may cause a malfunction of the islanding detection algorithm. To study the reliability of the proposed algorithm, a 1.5 kW induction motor is connected to the PCC via a switch in the non-islanding case. The simulation results of the induction motor starting are shown in Figure 10, and the experimental results of this condition are shown in Figure 11. At t = 1.5 s, the induction motor was started. The values of frequency and voltage nearly fixed, as shown in Figure 10(a) and (b) respectively, Figure 10(c) shows the ACOF value that its value does change but the value does not exceeds from threshold value at this time and Figure 10(d) shows the ROCOQAC value is not sensitive to motor switching, and its value does not large change within this time. Therefore, the proposed method does not send a trip and works in a reliable mode. In the experimental mode, the switching of the motor occurred at t = 1.0 s, and the voltage of the PCC decreased at this time as shown in Figure 11 (b). The voltage of grid in this study is 375 V and, at the instant of switching, decreased to 360 V. According to Figure11(c) and (d), it is obvious that the experimental results and simulation results prove the reliability of the proposed method.

Capacitor bank switching condition

Large capacitor bank switching in distribution power systems initiates disturbances. These disturbances are propagated in the distribution system and have some

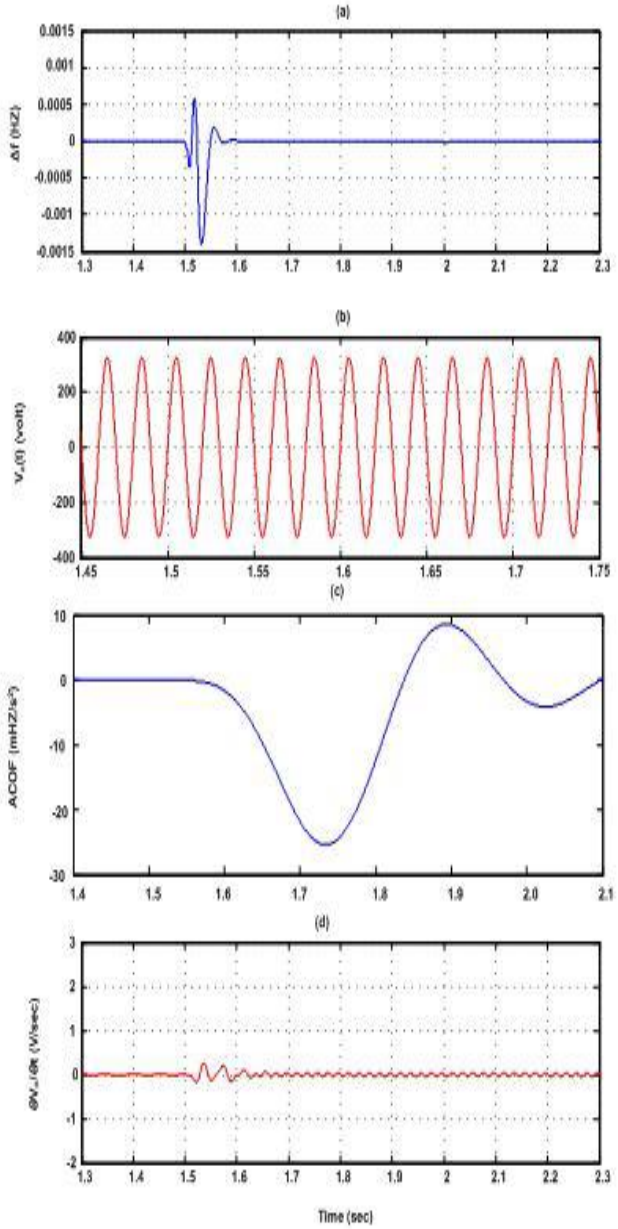

Figure 10. Dynamic response of the simulation system in motor starting condition , a) frequency of PCC, b) Instantaneous voltage of phase-a, c) accelerate of change of frequency, d) rate of change of q-component of voltage.

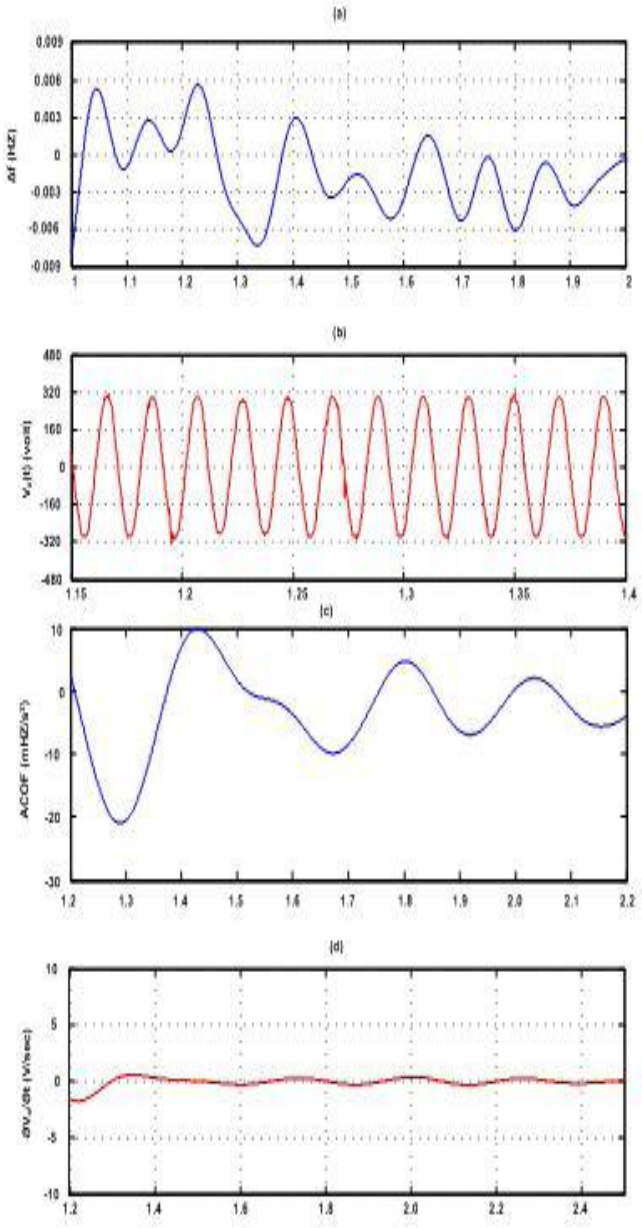

Figure 11. Dynamic response of the implementation system in motor starting condition , a) frequency of PCC, b) Instantaneous voltage of phase-a , c) accelerate of change of frequency, d) rate of change of q-component of voltage.

effects on the proposed method. To test the proposed algorithm, a large 2 kvar capacitor bank was switched at the PCC in the non-islanding case. This switching occurred at t = 1.5 s. The results for simulation system are shown in Figure 12. At the switching time, the voltage and frequency are almost constant. Figure 12 (c) and (d), shows that the ACOF and ROCOQAC do not change in this condition. The results show that ACOF and ROCOQAC do not have any sensitivity to the switching condition, and the proposed method works perfectly. The experimental results are described in Figure 13. A 2 kvar capacitor bank was switched at t = 2 s. The results confirm the simulation results.

Conclusion

This paper presents a new method based on frequency and voltage analysis (ACOF and ROCOQAC) for the islanding detection of wind turbines. The proposed

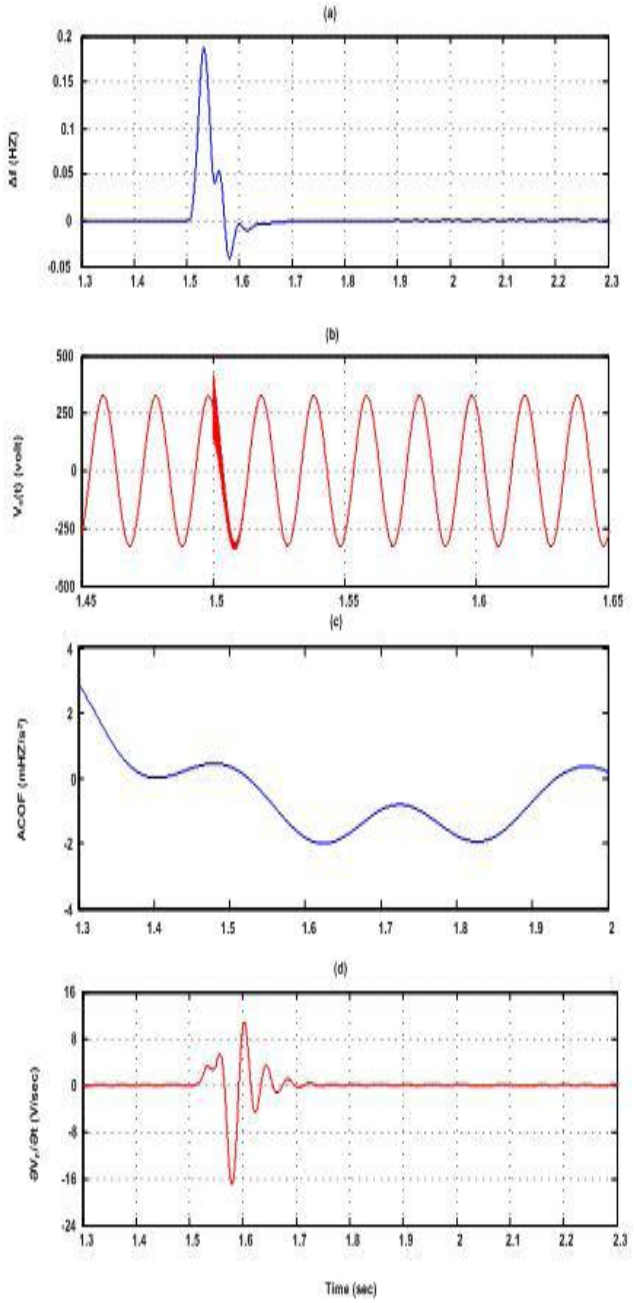

Figure 12. Dynamic response of the simulation system in capacitor switching condition, a) frequency of PCC, b) Instantaneous voltage of phase-a , c) accelerate of change of frequency, d) rate of change of q-component of voltage.

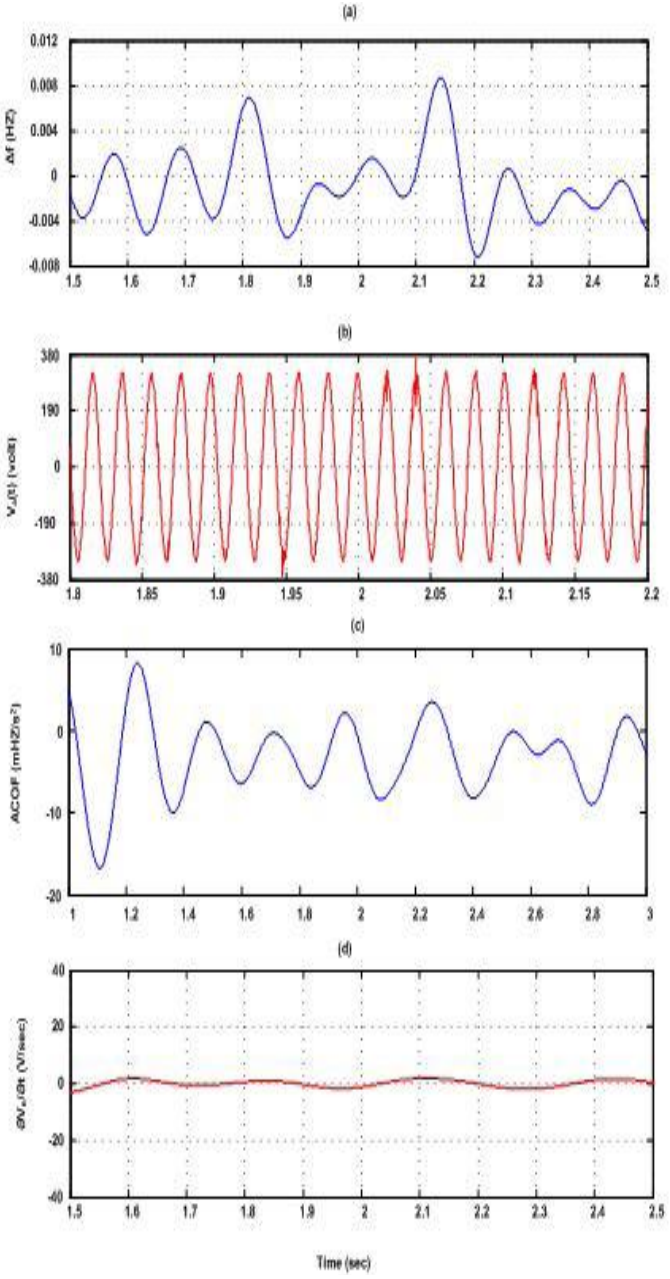

Figure 13. Dynamic response of the implementation system in capacitor switching condition, a) frequency of PCC, b) Instantaneous voltage of phase-a , c) accelerate of change of frequency, d) rate of change of q-component of voltage.

method was simulated and implemented on a wind turbine simulator. The results show the suitable reliability of the proposed method under different load conditions, such as capacitor bank switching and motor starting. Under these conditions, islanding detection is difficult. The method was able to detect the islanding condition of an induction generator type of a wind turbine within less than 0.2 s.

REFERENCES

Chowdhury SP, Chowdhury S, Crossley PA (2009). Islanding protection of active distribution networks with renewable distributed generators: A comprehensive survey. Electric Power Syst. Res. pp.1-9.

El-Arroudi K, Joós G, Kamwa I, McGillis DT (2007). Intelligent based approach to islanding detection in distributed generation. IEEE Trans. Power Deliv. 22(2):825-835.

Guillermo H, Reza I (2006). Current Injection for Active Islanding Detection of Electronically-Interfaced Distributed Resources. IEEE Tran. Power Deliv. 2006; 21(3):1698-1705.

http://www.renewableenergyworld.com/rea/news/article/2011/05/worldwind-outlook-down-but-not-out.
Jayaweera D, Galloway S, Burt G, McDonald JR (2007). A sampling approach for intentional islanding of distributed generation. IEEE Trans. Power Syst. 22(2):514-521.
Jiayi H, Chuanwen J, Rong X (2008). A review on distributed energy resources and MicroGrid. Renewable and Sustainable Energy Reviews 12:242–248.
Karimi H, Yazdani A, Iravani R (2008). Negative-sequence current injection for fast islanding detection of distributed resource unit. IEEE Trans. Power Deliv. 23(1):493-501.
Kazemi KH, Shataee A (2008). Islanding detection of wind farms by THD. IEEE Conf. DRPT2008 Nanjing China pp. 6-9.
Kunte SR, Gao W (2008). Comparison and review of islanding detection techniques for distributed energy resources. IEEE, Conf. pp. 1-8.
Swisher R, De Azua CR, Clendenin J (2001). Strong Winds on the Horizon: Wind Power Comes of Age. Proceedings of the IEEE, 89(12):1757-1764.
Vinod J, Zhihong Y, Amol K (2004). Investigation of Anti Islanding Protection of Power Converter Based Distributed Generators Using Frequency Domain Analysis. IEEE Trans. Power Electronics 19(5):1177-1183.
Wilsun X, Mauch K, Martel S (2004). An Assessment of DG Islanding Detection Methods and Issues for Canada CETC-Varennes. 2004-074 (TR) 411-INVERT, July, 2004.
Zeineldin HH, Abdel-Galil T, El-Saadany EF, Salama MMA (2007). Islanding detection of grid connected distributed generators using TLS-ESPRIT. Electric Power Syst. Res. 77:155–162.

academicJournals

Vol. 8(27), pp. 1417-1423, 23 July, 2013
DOI: 10.5897/IJPS2013.3946
ISSN 1992-1950 © 2013 Academic Journals
http://www.academicjournals.org/IJPS

International Journal of Physical Sciences

Full Length Research Paper

A method for placement of distributed generation (DG) units using particle swarm optimization

Noradin Ghadimi

Department of Electrical Engineering, Ardabil Branch, Islamic Azad University, Ardabil, Iran.

Accepted 19 July, 2013

Nowadays, the penetration of distributed generation (DG) in power networks takes special place worldwide and is increasing in developed countries. In order to improve voltage profile, stability, reduction of power losses etc, it is necessary that, this increasing of installation of DGs in distribution system should be done systematically. This paper introduces an optimal placement method in order to sizing and sitting of DG in IEEE 33 bus test system. The algorithm for optimization is particle swarm optimization (PSO). The proposed objective function is the multi objective function (MOF) that considers active and reactive power losses of the system and the voltage profile in nominal load of system. High performance of the proposed algorithm is proved by applying algorithm in 33 bus IEEE system using MATLAB software and in order to illustrate the feasibility of the proposed method optimization in three cases: one DG unit, Two DG units, and Three DG units- will achieved.

Key words: Distributed generation (DG), placement, particle swarm optimization, multi objective function (MOF), optimization.

INTRODUCTION

The anguish about rising environmental population and also the concern about the fossil fuels problems and limitations led to the installation of Distributed Generation (DG) which increases annually. In order to improve voltage profile, stability, reduction of power losses and etc, it is necessary that this increasing of installation of DGs in Distribution system should be systematically (Hedayati et al., 2008). The best choosing size and site of DGs in a distribution system is a complex optimization problem and if this problem contain the Multi Objective Function (MOF), this problem become much complex. Nowadays, meta heuristics optimization methods are being successfully applied to combinatorial optimization problems in distribution systems (Carmen and Djalma, 2006; Thong et al., 2007).

Gandomkar et al. (2005) determined the optimum location of the DG in the distribution network. The work was directed towards studying several factors related to the network and the DG itself such as the overall system efficiency, the system reliability, the voltage profile, the load variation, network losses, and the DG loss adjustment factors.

A Tabu search (TS) search method to find the optimal solution of their problem was explained by Katsigiannis and Georgilakis (2008), but the TS is known to be time consuming algorithm also it is may be trapped in a local minimum. In order to minimize the real power losses of power system in Lalitha et al. (2010), a Particle Swarm Optimization (PSO) algorithm was developed to specify the optimum size and location of a single DG unit. The problem was converted to an optimization program and the real power loss of the system was the only aspect considered in this study in order to determine optimally the location and size of only one DG unit.

E-mail: ghadimi.noradin@gmail.com. Tel: +98-914-702-8949.

El-Khattam et al. (2005), a deferent scenario was investigated to determine the optimum location of DG in order to modify the voltage profile and minimize the investment risk. The placement of one DG unit with specific size was explained by Ochoa et al. (2006). In this paper, MOF such as power line losses, modification of voltage profile, line loading capacity, and short circuit level were considered. P-V curves in Singh and Goswami (2010) have been used for analyzing voltage stability in electric power system to determine the optimum size and location of multiple DG units to minimize the system losses under limits of the voltage at each node of the system.

A genetic algorithm (GA) based fuzzy multi-objective approach for determining the optimum values of fixed and switched shunt capacitors was used to improve the voltage profile and maximize the net savings is proposed in Das (2008).

Particle Swarm Optimization (PSO) is used in this paper in order to find solution to optimization problems (Hashemi et al., 2011), optimal size and site of DG in 33-bus radial system of IEEE test system (Kashem et al., 2000). The aim of this paper is to proffer solution to sitting and sizing problem for optimization of MOF. Objective function of this paper is formed by combining on real power losses, reactive power reduction, voltage profile improving, and short circuit level improving of the mention system.

Problem formulation containing the objective function and constrains is explained in the next section. Section 3 presents the PSO algorithm in order to solve the optimization problem. The test system used to verify the effectiveness of the proposed technique is describe in Section 4 which explores the effectiveness of the proposed technique applied on simulation test system, Section 5 concludes the paper. The simulation test systems were simulated in MATLAB software.

PROBLEM FORMULATION

Objective functions formulation

As mentioned above, this paper introduces MOF optimization. The objective function was procured from the gather of each DG impact by the weighting factor assigned to that impact. This weighting factor is chosen by the planner to reflect the relative importance of each parameter in the decision making of sitting and sizing the DG. The DG location and its corresponding size in the distribution feeders can be optimally determined using the following objective function:

Max f (P_{loss},Q_{loss}, I_{SC},V_{level}).

Where:

$$f(P_{loss},Q_{loss},Isc,V_{level}) = w_1F_p + w_2F_q + w_3F_i + w_4F_v \quad (1)$$

F_p relates to increase of active power loss index in percent of system due to installation of DG which is given by:

$$F_p = \frac{P_{Loss}^{withoutDG} - P_{loss}^{withDG}}{P_{Loss}^{withoutDGl}} \quad (2)$$

Where, P_{Loss}^{withDG} is the real power loss in study system after installation of DG and $P_{Loss}^{withoutDG}$ is active power losses before installation.

F_q is a factor in order to determine the effect of DG in reactive power losses in mentioned system that given by:

$$F_q = \frac{Q_{Loss}^{withoutDG} - Q_{loss}^{withDG}}{Q_{Loss}^{withoutDGl}} \quad (3)$$

Where, Q_{Loss}^{withDG} and $Q_{Loss}^{withoutDG}$ are total reactive power losses in study system with installation DGs and without DGs respectively.

One of the avails of optimizes location and size of the DG is the improvement in voltage profile. This index penalizes the size-location pair which gives higher voltage deviations from the nominal value (Vnom). In this way, the closer the index to zero, the better is the network performance. The F_v can be defined as:

$$F_v = \max_{i=2}^{n}\left(\frac{|V_{nom}| - |V_i|}{|V_{nom}|}\right) \quad (4)$$

At last, in order to improve the short circuit level of system, F_I given in Equation 5, is gathered with the objective function:

$$F_I = \frac{I_{sc}^{withoutDG} - I_{sc}^{withDG}}{I_{sc}^{withoutDGl}} \quad (5)$$

The sum of the absolute values of the weights assigned to all impacts should add up to one as shown in the following equation:

$$|w_1| + |w_2| + |w_3| + |w_4| = 1 \quad (6)$$

The MOF in this paper in order to achieve the performance calculation of distribution systems for DG size and location is given by:

$$MOF = 0.4F_p + 0.2F_q + 0.15F_I + 0.25F_v \quad (7)$$

Constrains formulation

The MOF Equation 7 minimized is subjected to various operational constraints to satisfy the electrical requirements for distribution network. These constraints are the following.

Power-conservation limits

The algebraic sum of all incoming and outgoing power including line losses over the whole distribution network and power generated from DG unit should be equal to zero.

$$P_{Gen} + P_{DG} - \sum_{i=1}^{n} P_D - P_{total}^{Loss} = 0 \quad (8)$$

Distribution line capacity limits

Power flow through any distribution line must not exceed the thermal capacity of the line:

$$S_{ij} < S_{ij}^{\max} \quad (9)$$

Voltage limits

The voltage limits depend on the voltage regulation limits should be satisfied:

$$V_i^{\min} \le V_i \le V_i^{\max} \quad (10)$$

This paper employs PSO technique to solve the above optimization problem and search for the optimal or near optimal set of problem. Typical ranges of the optimized parameters are (0.01 to 100) KW for P_{DG} and (0.95-1.05) for voltage of buses.

PARTICLE SWARM OPTIMIZATION ALGORITHM

PSO was formulated by Edward and Kennedy in 1995 (Randy et al., 2004). The thought process behind the algorithm was inspired by the social behavior of animals, such as bird flocking or fish schooling. PSO is one of the most recent developments in the category of combinatorial met heuristic optimizations (Gaing, 2003). In PSO, each individual is referred to as a particle and represents a candidate solution to the optimization problem (Yoshida et al., 2000).

In first, a population of random solutions ‘‘particles’’ in a D-dimension space are composed. Each particle is a solution. The *i*th particle is represented by $X_i = (x_{i1}, x_{i2}, \ldots, x_{iD})$. Situation of each particle will be change in the next stage. The best situation of each particle will be determined by fitness function. If the fitness functions has a minimum value so far it is called best situation and save in $Pbest_i$. The global version of the PSO keeps track of the overall best value (gbest), and its location, obtained thus far by any particle in the population (Mandal et al., 2008). The particles update their velocities and positions based on the local and global best solutions. According to Equation 11, the velocity of particle *i* is represented as $V_i = (v_{i1}, v_{i2}, \ldots v_{iD})$. Acceleration is weighed by a random term, with separate random numbers being generated for acceleration toward pbest and gbest. The position of the *i*th particle is then updated according to Equation 12 (Binghui et al., 2007):

$$v_{id} = w \times v_{id} + c_1 \times rand() \times (P_{id} - x_{id}) + c_2 \times rand() \times (P_{gd} - x_{id}) \quad (11)$$

$$x_{id} = x_{id} + cv_{id} \quad (12)$$

Where, P_{id} and P_{gd} are pbest and gbest, c_1 and c_2 are constant values, ω will be determined by this equation:

ω_{max} and ω_{min} are the maximum and minimum value of ω respectively. At first ω start with large value that in the end of problem the value of the ω will be minimum.

In this optimization problem, the number of particles and the number of iterations are selected 30 and 40, respectively. Dimension of the particles will vary for each condition.

$$\omega = \omega_{\max} - \frac{\omega_{\max} - \omega_{\min}}{iter_{\max}} * iter \quad (13)$$

CASE STUDY AND PLACEMENT RESULTS

In this section, we illustrate that, DG placement affects the active power loss, reactive power losses and voltage profile. The placement of only a single DG, two DGs and three DGs are considered. In order to prove the efficiency of the proposed placement algorithm, IEEE 33-bus test system without tie lines that was presented in Kashem et al. (2000) as shown in Figure 1 is considered and the system details are given in Table 1.

In order to demonstrate variable number of DGs effect, we assume that, one-two and three DG unit which its size varying between 25 to 10 MW will be place in the mention network. The optimization results are given in Figure 2. This figure shows the value of MOF value in 40 iteration of PSO. From these results, it was obvious that the amount of MOF of the three DGs placement is least at the 40th iteration. The size and site location of one, two and three DGs are given in Table 2.

As can be seen from Table 2, the active power loss of the network without DG has maximum value and with three DG sitting have minimum amount and with comparing of power loss in four cases that is obvious that, the DG placement can has positive effect in power loss in the whole mention network.

Figure 3 illustrates buses voltage in four cases. With attention to this figure, the voltage profile with DG unit is better than without DG and the increasing number of DG unit’s affect the DGs in voltage profile become well.

In the next study, we assume that, three DG units in order to optimal placement are considered. The result of this study is represented by power system. The results of line power loss were presented in Table 2 and in this case this power loss becomes less than other cases and in Figure 4 the voltage profile is showed. The voltage profile in this case is better than the previous cases.

Conclusion

In this paper, a different approach based on PSO in order to multi objective optimization analysis, including one, two and three DG units, for size and site planning of DG in distribution system were presented. In solving this problem, at first problem was written in the form of the optimization problem which its objective function was defined and written in time domain and then the problem has been solved using PSO. The proposed optimization algorithm was applied to the 33-bus test system with tie lines.

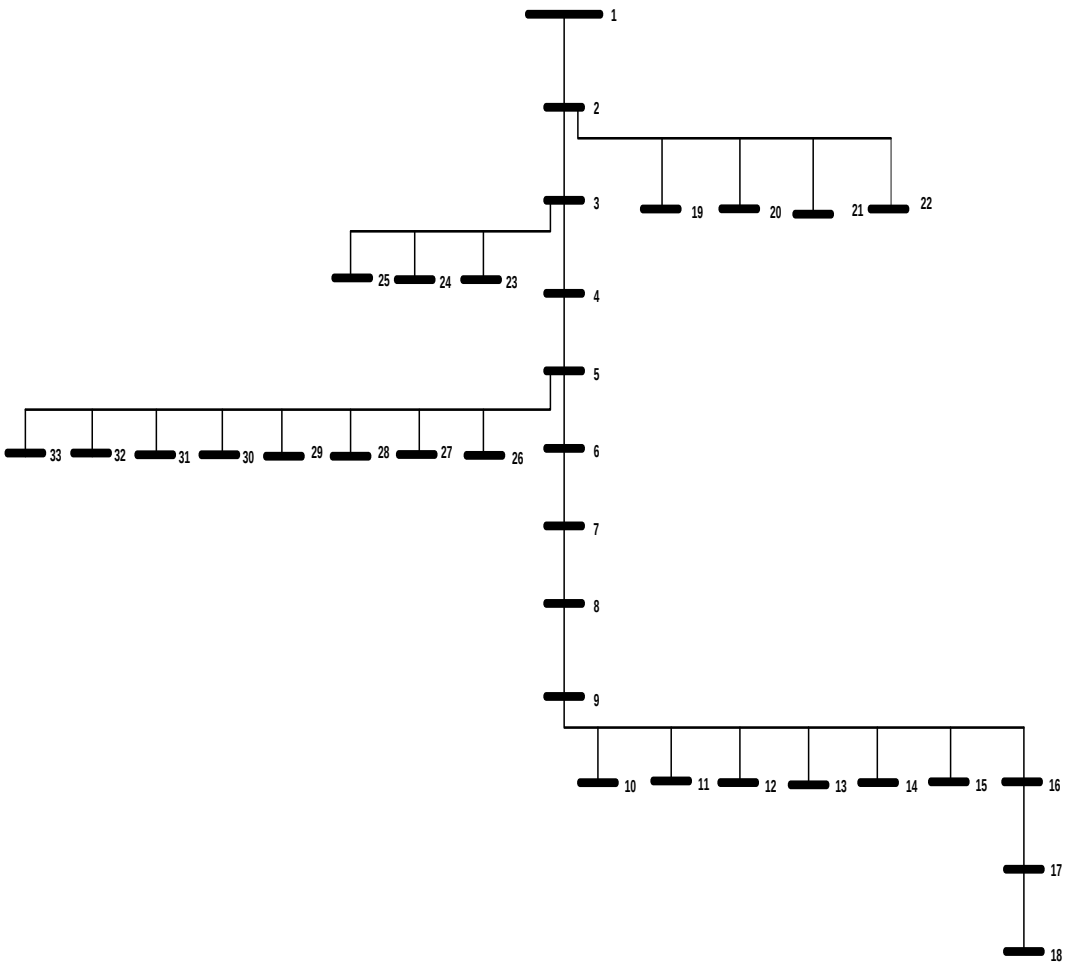

Figure 1. IEEE 33 bus study system with tie lines.

Table 1. Lines, active and reactive power details in study system.

Branch nom	Sen. node	Rec. node	Active power of rec. node KW	Reactive power of rec. node KVAr	Resistance ohms	Reactance ohms
1	1	2	100	60	0.0922	0.0470
2	2	3	90	40	0.4930	0.251 1
3	3	4	120	80	0.3660	0.1 864
4	4	5	60	30	0.3811	0.1941
5	5	6	60	20	0.8190	0.7070
6	6	7	200	100	0.1872	0.6188
7	7	8	200	100	1.7114	1.2351
8	8	9	60	20	1.0300	0.7400
9	9	10	60	20	1.0440	0.7400
10	10	11	45	30	0.1966	0.0650
11	11	12	60	35	0.3744	0.1238
12	12	13	60	35	1.4680	1.1550
13	13	14	120	80	0.5416	0.7129
14	14	15	60	10	0.5910	0.5260
15	15	16	60	20	0.7463	0.5450

Table 1. Contd.

16	16	17	60	20	1.2890	1.7210
17	17	18	90	40	0.7320	0.5740
18	2	19	90	40	0.1640	0.1565
19	19	20	90	40	1.5042	1.3554
20	20	21	90	40	0.4095	0.4784
21	21	22	90	40	0.7089	0.9373
22	3	23	90	50	0.4512	0.3083
23	23	24	420	200	0.8980	0.7091
24	24	25	420	200	0.8960	0.7011
25	5	26	60	25	0.2030	0.1034
26	26	27	60	25	0.2842	0.1447
27	27	28	60	20	1.0590	0.9337
28	28	29	120	70	0.8042	0.7006
29	29	30	200	600	0.5075	0.2585
30	30	31	150	70	0.9744	0.9630
31	31	32	210	100	0.3105	0.3619
32	32	33	60	40	0.3410	0.5302

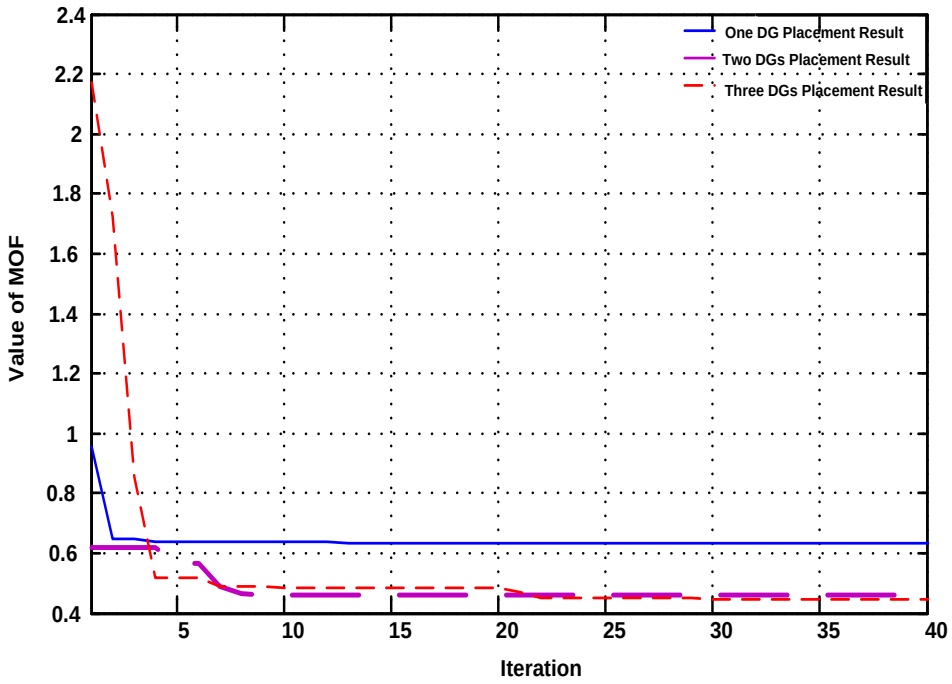

Figure 2. Value of MOF for one, two and three DGs.

Table 2. Optimum results of PSO for location and size of DGs.

Number of DG	DG size			DG site			Network loss
Without DG	-			-			0.8920
One DG	1136.6			11			0.6340
Two DGs	1143.2	1044.2		24	11		0.4583
Three DGs	1700.1	668.7	506.0	3	8	15	0.4436

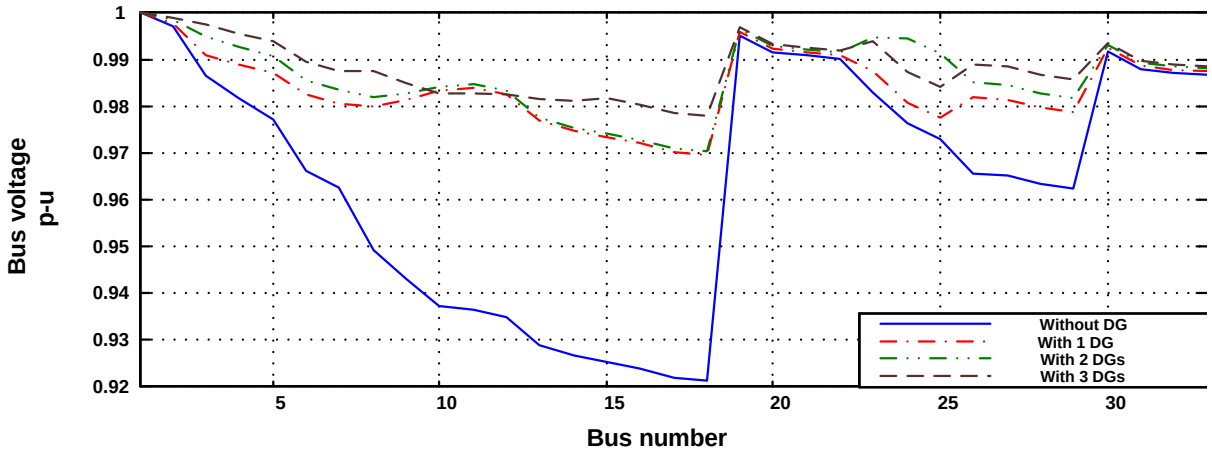

Figure 3. Voltage profile of study system with three DG units, two DG units, single DG unit, and without DG.

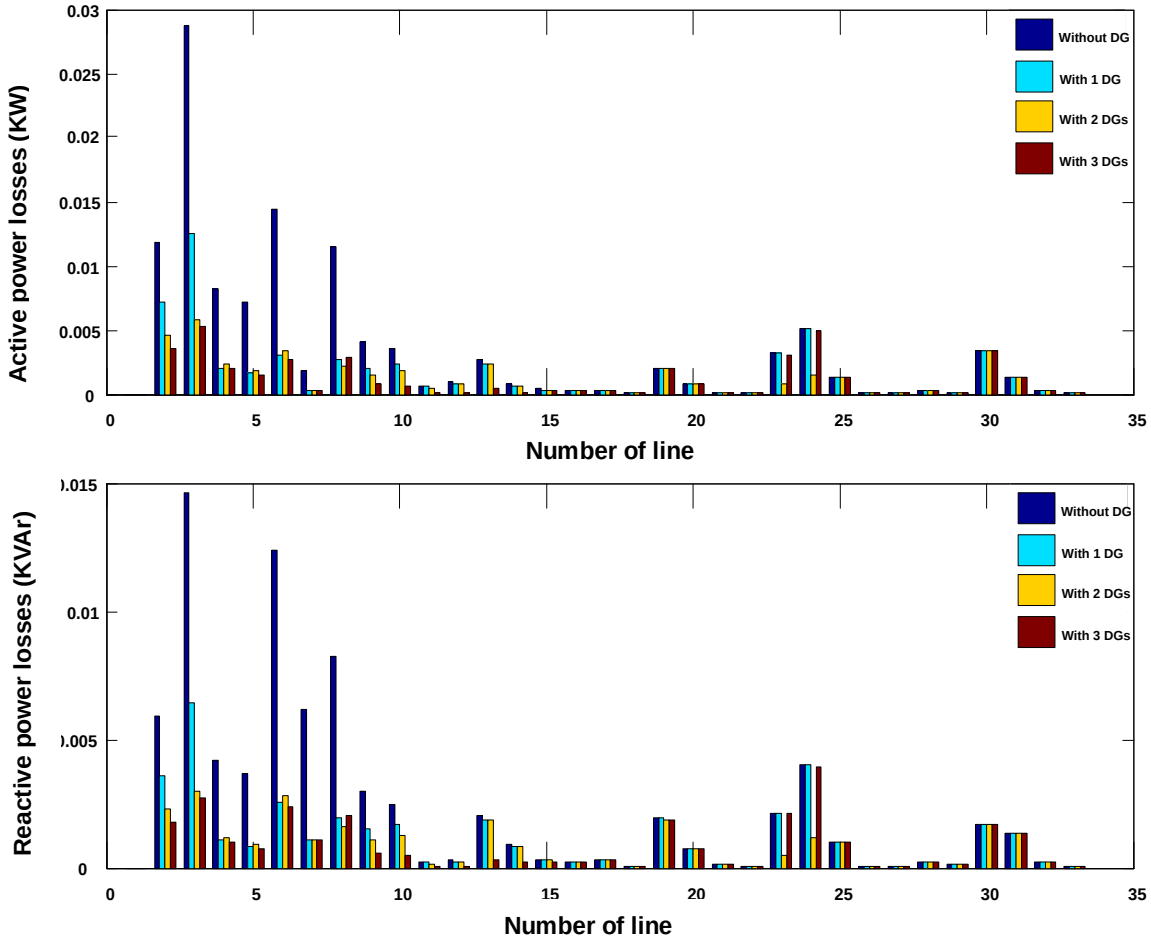

Figure 4. Active and reactive of lines with three DG units, two DG units, single DG unit and without DG.

The results clarified the efficiency of this algorithm for the improvement of voltage profile and reduction of power losses in study system.

REFERENCES

Binghui Y, Xiaohui Y, Jinwen W (2007). Short-term hydro-thermal scheduling using particle swarm optimization method. Energy

Convers. Manage. 48:1902-1908.
Carmen LTB, Djalma MF (2006). Optimal distributed generation allocation for reliability, losses, and voltage improvement. Elect. Power Energy Syst. 28:413-420.
Das D (2008). Optimal placement of capacitors in radial distribution system using a Fuzzy-GA method'. Elect. Power Energy Syst. 30:361-367.
El-Khattam W, Hegazy YG, Salama MMA (2005). "An integrated distributed generation optimization model for distribution system planning". IEEE Trans. Power Syst. 20(2):1158-1165.
Gaing Z (2003). Particle swarm optimization to solving the economic dispatch considering the generator constraints, IEEE Trans. PWRS. 18(3):1187-1195.
Gandomkar M, Saveh AU, Vakilian M, Ehsan M (2005). Acombination of genetic algorithm and simulated annealing for optimal DG allocation in distribution networks, in: Proc. IEEE Electr. Comput. Eng. Can. Conf. 1-4:645-648.
Hashemi F, Alizade AR, Zebardast SJ, Ghadimi N (2011). "Determining the optimum cross-sectional area of the medium voltage feeder for loss reduction and voltage profile improvement based on particle swarm algorithm" 10th Int. Conf. Environ. Elec. Eng. (EEEIC), 8–11:813-817.
Hedayati HS, Nabaviniaki A, Akbarimajd A (2008). "A method for placement of DG units in distribution networks", IEEE Trans. Power Deliver. 23(3):1620-1628.
Kashem MA, Ganapathy V, Jasmon GB, Buhari MI (2000). A Novel Method for Loss Minimization in Distribution Networks, International Conference on Electric Utility Deregulation and Restructuring and Power Technologies 2000, London, 4-7 April. pp. 251-256.
Katsigiannis YA, Georgilakis PS (2008). "Optimal sizing of small isolated hybrid power systems using tabu search". J. Optoelectron. Adv. Mater. 10(5):1241-1245.
Lalitha MP, Reddy VCV, Usha V (2010). "Optimal DG Placement for Minimum Real Power Loss in Radial Distribution Systems Using PSO". J. Theor. Appl. Inform. Technol. pp. 107-116.
Mandal KK, Basu M, Chakraborty N (2008). Particle swarm optimization technique based short-term hydrothermal scheduling. Appl. Soft Comput. 8:1392-1399.
Ochoa LF, Padilha-Feltrin A, Harrison GP (2006). "Evaluating distributed generation impacts with a multiobjective index". IEEE Trans. Power Deliver. 21(3):1452-1458.
Randy LH, Sue EH (2004). PRACTICAL GENETIC ALGORITHMS, Wiley & Sons, Inc., Hoboken, New Jersey.
Singh RK, Goswami SK (2010). "Optimum allocation of distributed generations based on nodal pricing for profit, loss reduction and voltage improvement including voltage rise issue". Int. J. Elect. Power Energy Syst. 32:637-644.
Thong VV, Driesen J, Belmans R (2007). "Transmission system operation concerns with high penetration level of distributed generation", in Proc. of Inter. Universities Power Engineering Conference, Brighton. pp. 867-871.
Yoshida H, Kawata K, Fukuyama Y, Takayama S, Nakanishi Y (2000). A particle swarm optimization for reactive power and voltage control considering voltage security assessment. IEEE Trans. PWRS. 15(4):1232-1239.

academicJournals

Vol. 8(27), pp. 1424-1436, 23 July, 2013
DOI: 10.5897/IJPS2013.3947
ISSN 1992-1950 © 2013 Academic Journals
http://www.academicjournals.org/IJPS

International Journal of Physical Sciences

Full Length Research Paper

Adaptive neuro-fuzzy inference system (ANFIS) islanding detection based on wind turbine simulator

Noradin Ghadimi* and Behrooz Sobhani

Department of Electrical Engineering, Ardabil Branch, Islamic Azad University, Ardabil, Iran.

Accepted 19 July, 2013

This paper presents a passive islanding detection method based on means of a neuro-fuzzy approach for wind turbines. Several methods based on passive and active detection scheme have been proposed. While passive schemes have a large Non detection zone (NDZ), concern has been raised on active method due to its degrading power quality effect. Reliably detecting this condition is regarded by many as an ongoing challenge as existing methods are not entirely satisfactory. The proposed method is based on voltage measurements and processing of the hybrid intelligent system called the Adaptive neuro-fuzzy inference system (ANFIS) for islanding detection. This new method based on passive methods will help to reduce the NDZ without any perturbation that deteriorates the output power quality opposite active methods. This method detects the islanding conditions with the analysis of these signals. The studies reported in this paper are based on an experimental system (wind turbine simulator). The results showed that, the ANFIS-based algorithm detects islanding situation accurate than other islanding detection algorithms. Moreover, for those regions which are in need of a better visualization, the proposed approach would serve as an efficient aid such that the mains power disconnection can be better distinguished.

Key words: Distributed generation, islanding detection, non detection zone, adaptive neuro fuzzy inference system, fuzzy subtractive clustering.

INTRODUCTION

The increase of distributed resources in the electric utility systems is indicated due to recent and ongoing technological, social, economical and environmental aspects. Distributed generation (DG) units have become more competitive against the conventional centralised system by successfully integrating new generation technologies and power electronics. Hence, it attracts many customers from industrial, commercial, and residential sectors. DGs generally refer to Distributed Energy Resources (DERs), including photovoltaic, fuel cells, micro turbines, small wind turbines, and additional equipment (Jiayi et al., 2008). The total global installed wind capacity at the end of 2010 was 430 TWh annually, which is 2.5% of the total global demand. Based on the current growth rates, World Wide Energy Association (WWEA) predicts that, in 2015, a global capacity of 600 GW is possible. By the end of the year 2020, at least 1500 GW can be expected to be installed globally (http://www.renewableenergyworld.com/rea/news/article/2011/05/worldwind). However, connecting wind turbines to distribution networks produces some problems, such as islanding.

Islanding when occurred, DG and its local load become electrically isolated from the utility grid (Behrooz et al., 2011). However, the wind turbine produces electrical energy and supplies the local load. Islanding creates

*Corresponding author. E-mail: noradin.ghadimi@gmail.com.

many problems in system and causes the existing standards not to permit DGs to be utilized in islanding mode (Smith et al., 2000). Some of these reasons are:

i) Create safety hazard for personals,
ii) Power quality problems for customers load,
iii) Overload condition of wind turbine generator,
iv) Out of phase recloser connection (Vachtsevanous and Kang, 1989; Zeineldin et al., 2006).

Thus, islanding conditions should be detected and interrupted. This application should be done in less than 2 s (Vachtsevanous and Kang, 1989). Originally, the methods of islanding detections are divided to two methods: communication methods and local methods

Local methods have been classified as active and passive techniques (Smith et al., 2000). Active techniques are based on directly interact with the on-going power system operation, such as impedance measurement (IEEE, 2003), frequency shift, active frequency drift (IEEE, 2003), sandia frequency shift (IEEE, 2003; Karimi et al., 2008) sandia voltage shift (IEEE, 2003; Karimi et al., 2008), phase shift, current injection (Hernandez-Gonzalez and Iravani, 2006), negative sequence current injection method (IEEE, 1999). Passive techniques are based on measurement and information at the local site, such as under/over frequency (IEEE, 2003), under/over voltage (IEEE, 2003), voltage phase jump, voltage unbalanced and total harmonic distortion (http://www.renewableenergyworld.com/rea/news/article/2011/05/worldwind), rate of change of frequency (Hung et al., 2003), vector surge (Hung et al., 2003; Hopewell et al., 1996), phase displacement monitoring (Hopewell et al., 1996), rate of change of generator power output (IEEE, 2003), comparison of rate of change of frequency (Imece et al., 1989).

In this paper, a new method based on Discrete Wavelet Transform (DWT) has been proposed for islanding detection of wind turbines. The proposed technique, which is suitable for asynchronous DGs, is explained in Section 3. Section 4 explains the simulation and experimentally test system used to verify the effectiveness of the proposed technique. Section 5 explores the effectiveness of the proposed technique applied on simulation and experimentally test system, Section 6 concludes the paper. The simulation test systems were simulated in MATLAB/ SIMULINK using SimPowerSystemBlockSet. Simulation and experimentally results show that, the proposed islanding detection technique works well in discriminating between switching and islanding conditions.

Adaptive neuro-fuzzy inference system (ANFIS)

Artificial intelligence, including neural network, Fuzzy logic (FL) inference (Gupta and Rao, 1994; Yen et al., 1995) has been used to solve many nonlinear classification problems. The main advantages of a Fuzzy logic system (FLS) are the capability to express nonlinear input/output relationships by a set of qualitative if-then rules. The main advantage of a neural network (NN), on the other hand, is the inherent learning capability, which enables the networks to adaptively improve its performance. The key properties of neuro-fuzzy network are the accurate learning and adaptive capabilities of the neural networks, together with the generalization and fast learning capabilities of FLS. The ANFIS is a very powerful approach for modeling nonlinear and complex systems with less input and output training data with quicker learning and high precision. ANFIS is an adaptive network which permits the usage of neural network topology together with FL. It not only includes the characteristics of both methods, but also eliminates some disadvantages of their lonely-used case. Basically a Fuzzy inference system (FIS) is composed of five functional blocks (Figure 1).

Operation of ANFIS looks like feed-forward back propagation network. Consequent parameters are calculated forward while premise parameters are calculated backward. There are two learning methods in neural section of the system: Hybrid learning method and back-propagation learning method. In fuzzy section, only zero or first order Sugeno inference system or Tsukamoto inference system can be used. The ANFIS approach learns the rules and membership functions from data. The objective of ANFIS is to adjust the parameters of a fuzzy system by applying a learning procedure using input-output training data.

The basic structure of the type of FIS is a model that, maps input characteristics to input membership functions, input membership function to rules, rules to a set of output characteristics, output characteristics to output membership functions, and the output membership function to a single-valued output or a decision associated with the output.

This section introduces the basics of ANFIS network architecture and its hybrid learning rule. The Sugeno fuzzy model was proposed by Takagi, Sugeno, and Kang in an effort to formalize a systematic approach to generating fuzzy rules from an input-output dataset. A typical fuzzy in a Sugeno fuzzy model has the format:

If x is A and y is B then z = f (x, y)

Where A and B are fuzzy sets in the antecedent; z = f(x,y) is a crisp function in the consequent. Usually f(x, y) is a polynomial in the input variable x and y, but it can be any other functions that can appropriately describe the output of the system within the fuzzy region specified by the antecedent of the rule. When f(x, y) is a first-order polynomial, this first order sugeno fuzzy model is proposed in sugeno (1998). When f is a constant, then, the zero order Sugeno fuzzy model, which is functionally

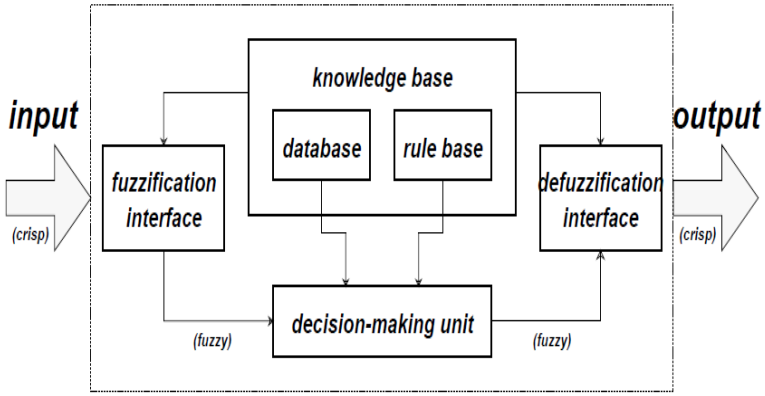

Figure 1. Fuzzy inference system.

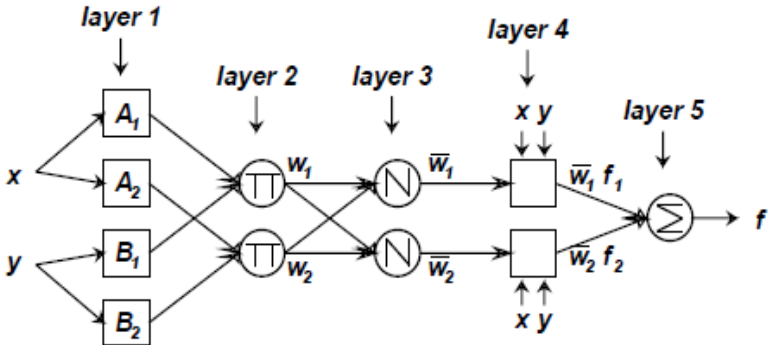

Figure 2. ANFIS architecture.

equivalent to a radial basis function network under certain minor constraints. The architecture of ANFIS with two inputs, one output and two rules is given in Figure 2. In this connected structure, the input and output nodes represent the training values and the predicted values, respectively, and in the hidden layers, there are nodes functioning as membership functions (MFs) and rules. This architecture has the benefit that, it eliminates the disadvantage of a normal feed forward multilayer network, where it is difficult for an observer to understand or modify the network. Here *x*, *y* are inputs, F is output, the circles represent fixed node functions and squares represent adaptive node functions.

Consider a first order Sugeno FIS which contains two rules:

Rule 1: If X is Al and Y is B1, then f1 = P1x + q1y+r1
Rule 2: If X is A2 and Y is B 2 then f2 = P2x + q2y+r2

Where, P1, P2, q1, q2, r1, andr2 are linear parameters and A1, A2, B1, and B2 are nonlinear parameter. ANFIS is an implementation of a FL inference system with the architecture of a five-layer feed-forward network. The system architecture consists of five layers, namely, fuzzy layer, product layer, normalized layer, de-fuzzy layer and total output layer. With this way, ANFIS uses the advantages of learning capability of neural networks and inference mechanism similar to human brain provided by FL. The operation of each layer is as follows: Here the output node *i* in layer *l* is denoted as O_i^l .

Layer 1 is the fuzzification layer. Every node *i* in this layer is an adaptive node with node function:

$$O_i^1 = \mu_{A_i}(x), \quad O_{i+2}^1 = \mu_{B_i}(y) \quad i = 1,2 \tag{1}$$

Where, *x* is the input to i_{th} node, O_i^l is the membership grade of *x* in the fuzzy set *Ai*. Generalized bell membership function is popular method for specifying fuzzy sets because of their smoothness and concise notation, and defined as:

$$\mu_{A_i}(x) = \frac{1}{1+\left|\frac{x-c_i}{a_i}\right|^{2b_i}} \tag{2}$$

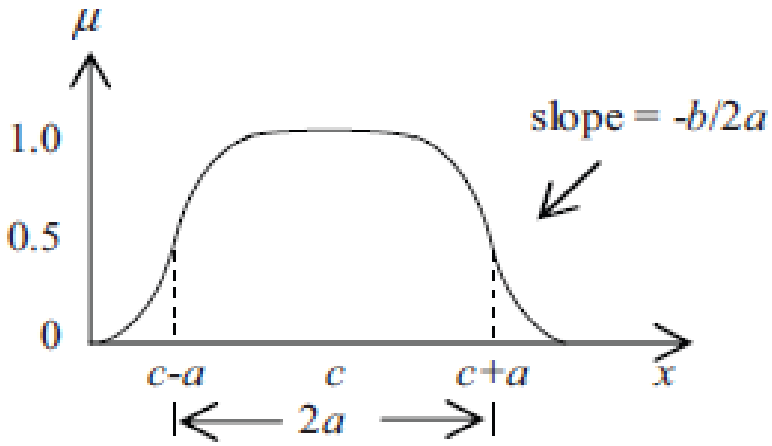

Figure 3. Generalized bell function.

Here $\{a_i, b_i, c_i\}$ is the parameter set of the membership function. The center and width of the membership function is varied by adjusting c_i and a_i. The parameter b_i is used to control the slopes at the crossover points. Figure 3 shows the physical meaning of each parameter in a generalized bell function. The parameters in this layer are called premise parameters. This layer forms the antecedents of the fuzzy rules (*IF* part).

Layer 2 is the rules layer. Every node in this layer is a fixed node and contains one fuzzy rule. The output is the product of all incoming signals and represents the firing strength of each rule:

$$O_i^2 = w_i = \mu_{A_i}(x)\mu_{B_i}(y), \quad i = 1,2 \tag{3}$$

Layer 3 is the normalization layer. Every node in this layer is a fixed node and i_{th} node calculates the ratio of i_{th} rule's firing strength to the sum of all rules' firing strengths. Outputs of this layer are called normalized firing strengths computed as:

$$O_{3,i} = \overline{w}_i = \frac{w_i}{w_1 + w_2} \quad i = 1,2 \tag{4}$$

Layer 4 is the consequent layer. Every node in this layer is an adaptive node and computes the values of rule consequent (then part) as:

$$O_i^4 = \overline{w}_i f_i = \overline{w}_i (p_i x + q_i y + r_i) \tag{5}$$

Here w_i is the output of Layer 3 and the parameters $\{p_i, q_i, r_i\}$ are known as consequent parameters. Layer 5 is the summation layer and it consists of single fixed node which calculates the overall output as the summation of all incoming signals as:

$$O_i^5 = \sum_i \overline{w}_i f_i = \frac{\sum_i w_i f_i}{\sum_i w_i} \tag{6}$$

ROPOSED DETECTION ALGORITHM

In this study, we propose to use a hybrid intelligent system called ANFIS for islanding detection. We combine the ability of a NN to learn with FL to reason in order to form a hybrid intelligent system called ANFIS.

ANFIS training algorithm can be efficiently used to build fuzzy rules from correct input-output numerical data pairs. The main motivations for such an investigation are:

i) The ANFIS is a well known and successful solution
ii) It can be used directly on the data recorded in the learning stage, and so it can be further considered for a real-time implementation
iii) It stands as a classical algorithm, with trustful implementation as the one included in MATLAB.

More specifically, in the forward pass of the hybrid learning algorithm, node outputs go forward until layer 4 and the consequent parameters are identified by the least-squares method. In the backward pass, the error signals propagate backwards and the premise parameters are updated by gradient descent. We don't necessarily have a predetermined model structure based on characteristics of variables in our system. There will be some modeling situations in which we can't just look at the data and discern what the membership functions should look like. Rather than choosing the parameters associated with a given membership function arbitrarily, these parameters could be chosen so as to tailor the membership functions to the input-output data in order to account for these types of variations in the data values.

These techniques provide a method for the fuzzy modeling procedure to learn information about a data set, in order to compute the membership function parameters that best allow the associated FIS to track the given input/output data. Using a given input/output

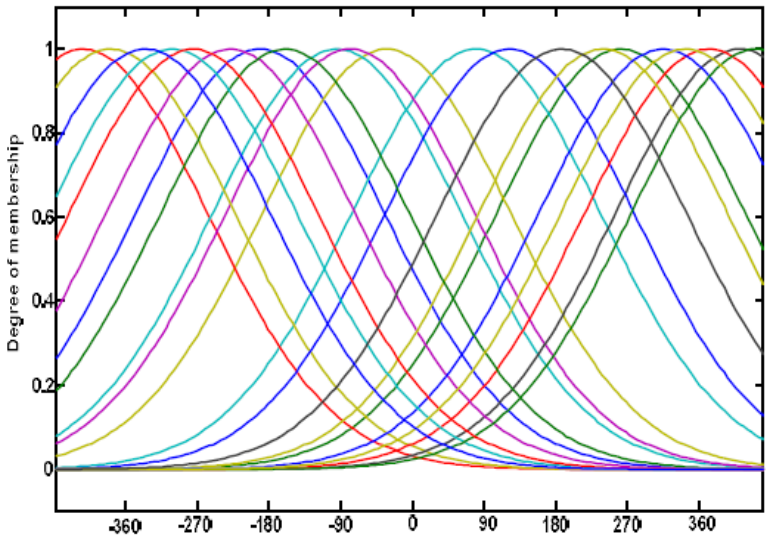

Figure 4. Membership function.

data set, the ANFIS constructs a FIS whose membership function parameters are tuned (adjusted) using either a back propagation algorithm. This allows our fuzzy systems to learn from the data they are modeling.

The proposed approach is based on the passive method of islanding detection considering the data clustering approach. In addition, this method includes building a simplified and robust fuzzy classifier initialized by the subtractive clustering and makes a FIS for islanding detection. As a result of the increasing complexity and dimensionality of classification problems, it becomes necessary to deal with structural issues of the identification of classifier systems. Important aspects are the selection of the relevant features and determination of effective initial partition of the input domain. The purpose of clustering is to identify natural groupings of data to produce a concise representation of a system's behavior. Subtractive clustering is a fast, one-pass algorithm for estimating the number of clusters and the cluster centers in a set of data.

In this paper, an ANFIS models which takes voltage signal as inputs and islanding condition as output. Firstly, voltage data taken from the DG for provide a dataset. The next step, construct a FIS that could best predict the islanding condition or normal condition. ANFIS training can use alternative algorithms to reduce the error of the training. A combination of the gradient descent algorithm and a least squares algorithm is used for an effective search for the optimal parameters. The main benefit of such a hybrid approach is that, it converges much faster, since it reduces the search space dimensions of the back propagation method used in neural networks. ANFIS was trained with the first half epochs and the next half epochs were used for validation. The Root mean squared error (RMSE) from each of the validating epochs was calculated. Averages of RMSE per patient were calculated for all patients to give the average RMSE. Thus before training a FIS, the data set has been divided into training set and test sets. The training set is used to train a fuzzy mode, while the test set is used to determine when training should be terminated to prevent over fitting. After training, for verify the model FIS we calculate, the RMSE of the system generated by the training data that, it is equal to 0.1068. To validate the generalize ability of the model; we apply test data to the FIS that, it is equal 0.018. Figure 4 shows the membership function obtained only from dataset for all conditional of islanding and normal operation without any setting of threshold for islanding detection parameter. In this paper, we can overcome the problem of setting the detection thresholds for islanding detection.

ANFIS models takes voltage as inputs and islanding condition as output. If the islanding is detected, the output ANFIS is higher than 0.6. Conversely, if the islanding is not detected, the output ANFIS is around 0 or less than 0.5. The result obtained indicates that, ANFIS is effective method for islanding detection.

CASE STUDY

Figure 5 shows a schematic diagram of a wind turbine unit. The DG unit is a wind turbine induction generator, and a capacitor bank is used to improve the power factor. The local load is a three-phase parallel RL before the circuit breaker (CB), in which "r" denotes the series resistance inductance and V_f indicates the voltage drop across the parallel load. The parallel RL is conventionally adopted as the local load for the evaluation of islanding detection methods when the load inductance is tuned to the system frequency. This system, as shown in Figure 5, is connected to a Point of Common Coupling (PCC) with a step-up transformer. To obtain the experimental results, a wind turbine simulator, as shown in Figure 6, was implemented. Figures 7 and 8 showed the implemented simulator system. The implemented system parameters are given in Table 1. The parallel load inductance is considered infinite. Thus, the parallel load is only a resistance, and hence the unit of "L" is "inf". Figure 9 shows the motor saturation curve. In the grid-connected condition, the switches SW1 and SW2 are closed. The islanding condition occurs when SW2 is open.

The voltage and frequency of DG should have admissible values in both grid-connected and islanded modes. In the grid-connected mode, the voltage magnitude and frequency of the local load at the PCC are regulated by the grid.

IMPLEMENTATION RESULTS

In this study, the simulation is conducted in four scenarios to illustrate the effectiveness of the proposed method.

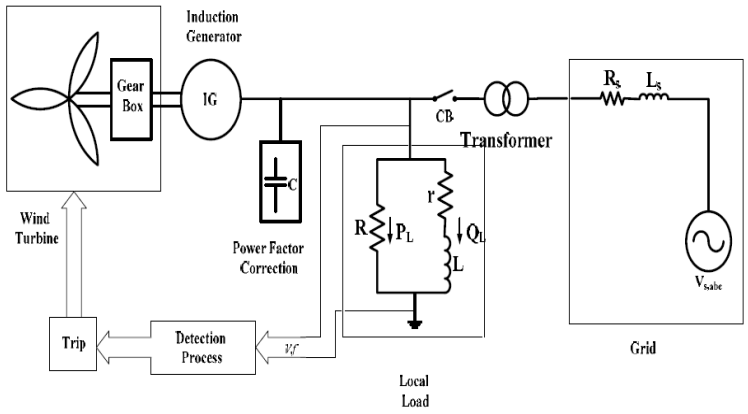

Figure 5. Single line diagram of study system.

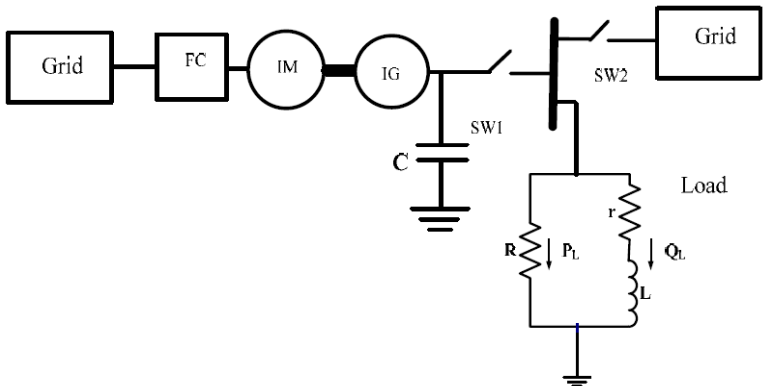

Figure 6. Single line diagram of implementation system in order to islanding condition detection.

Figure 7. Implementation system in order to islanding condition detection.

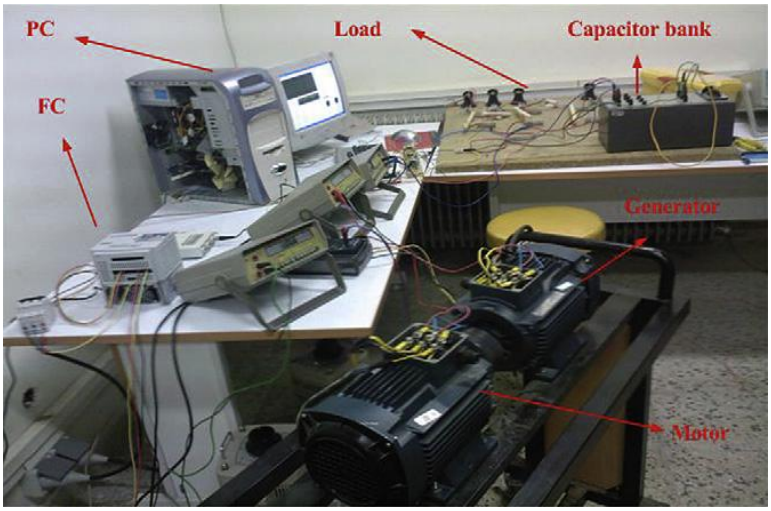

Figure 8. Implementation system in order to islanding condition detection.

Table 1. Parameters of the implemented system.

Parameter		Value
Induction motors	Sn	2 KVA
	Vn	400 V
	F	50 HZ
	PF	0.78 Lag
	Rs, Rr	2.3541 Ω
	Lr, Ls	0.01678 H
	Lm	0.275 H
Local load	R	180 Ω
	L	Inf
Capacitor	C	36.75 µF

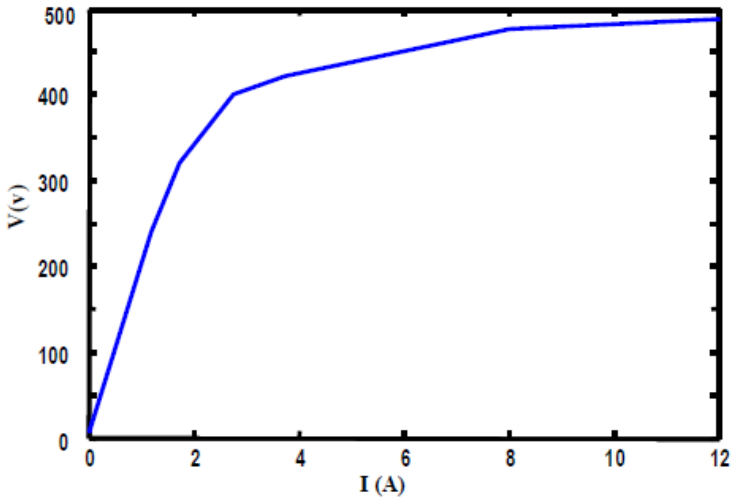

Figure 9. Motor and generator saturation curves.

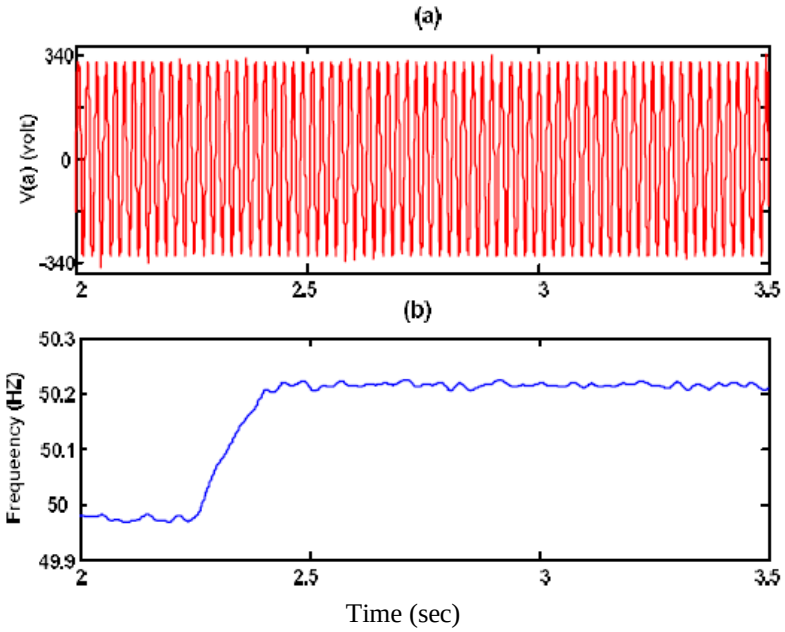

Figure 10. Match power condition: (a) phase voltage, (b) frequency.

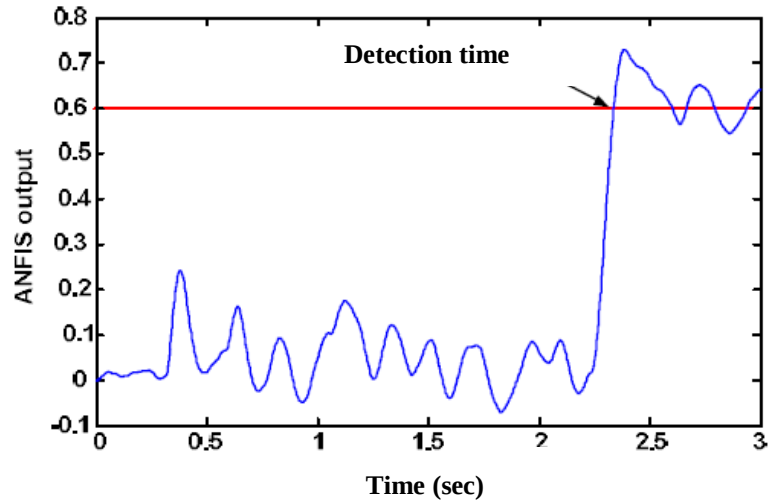

Figure 11. ANFIS output for match power conditional.

Match power condition

In this test, the active and reactive power of local load is 0.8 KW and 0Kvar, respectively. The value of capacitor is 36.0 μF, the distributed generator is assumed to separate from the grid, where the event is assumed to take place at 2.2 s. In Figure 10a and b, the waveforms of phase voltage and frequency of DGs are individually depicted. Immediately following this loss of utility, proposed method relay fails to detect islanding condition. Figure 11 shows the output of proposed method algorithm result. ANFIS output is rich to above “0.5” value which leads to islanding detection. So the ANFIS based protection algorithm produced the trip signal and sends it to DG.

Mismatch power condition

At first, the amount of capacitor bank is lesser than nominal condition. The active power set to 0.66 KW and reactive power set to 0.1 Kvar, respectively. The distributed generator is assumed to separate from the

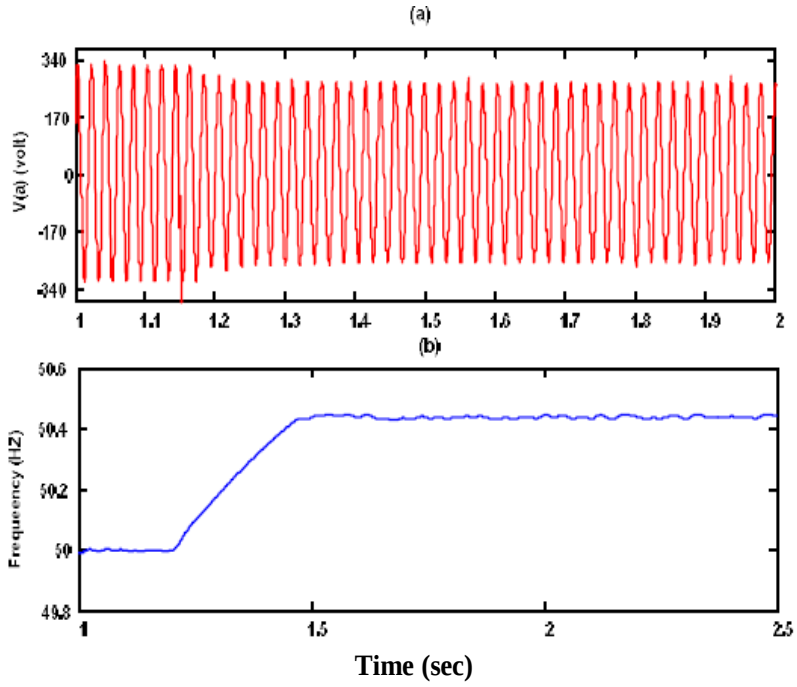

Figure 12. Mismatch power condition: (a) three phase voltage, (b) frequency.

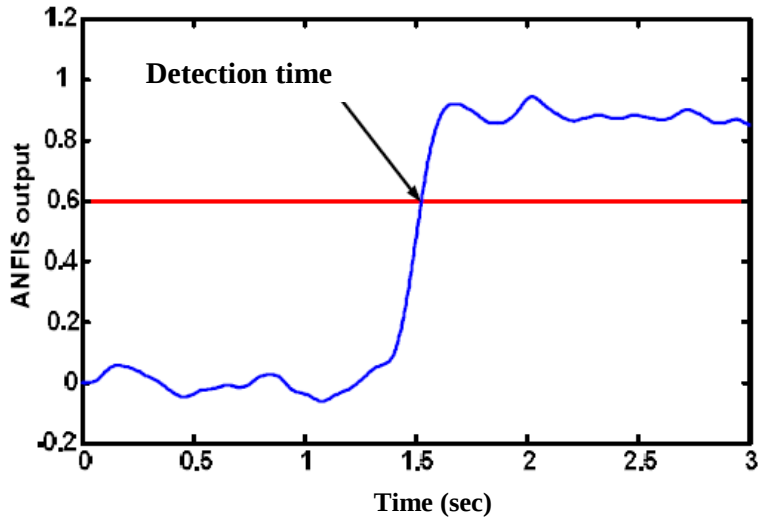

Figure 13. ANFIS output for Mismatch power condition.

grid, where the event is assumed to take place at 1.15 s. In Figure 12a and b, the waveforms of phase voltage and frequency of DGs are individually depicted. Immediately following this loss of utility, frequency is increase and voltage is drop. Figure 13 shows the ANFIS output that is rich to higher than “0.5” value which leads to islanding detection. So the ANFIS based protection algorithm produced the trip signal and sends to DG.

At the next test, the amount of capacitor bank is higher than nominal condition and set to 40 μF. The active power set to 0.66 KW and reactive power set to 0.1 Kvar, respectively. After islanding event at 2.6 s, Figures 14a and b and c shows the waveforms of instantaneous phase voltage, RMS phase voltage and frequency of DGs, respectively. As can be seen, frequency is drop and voltage is increase. Figure 15 shows the ANFIS output that is rich to higher than “0.5” value which leads to islanding detection. So the ANFIS based protection

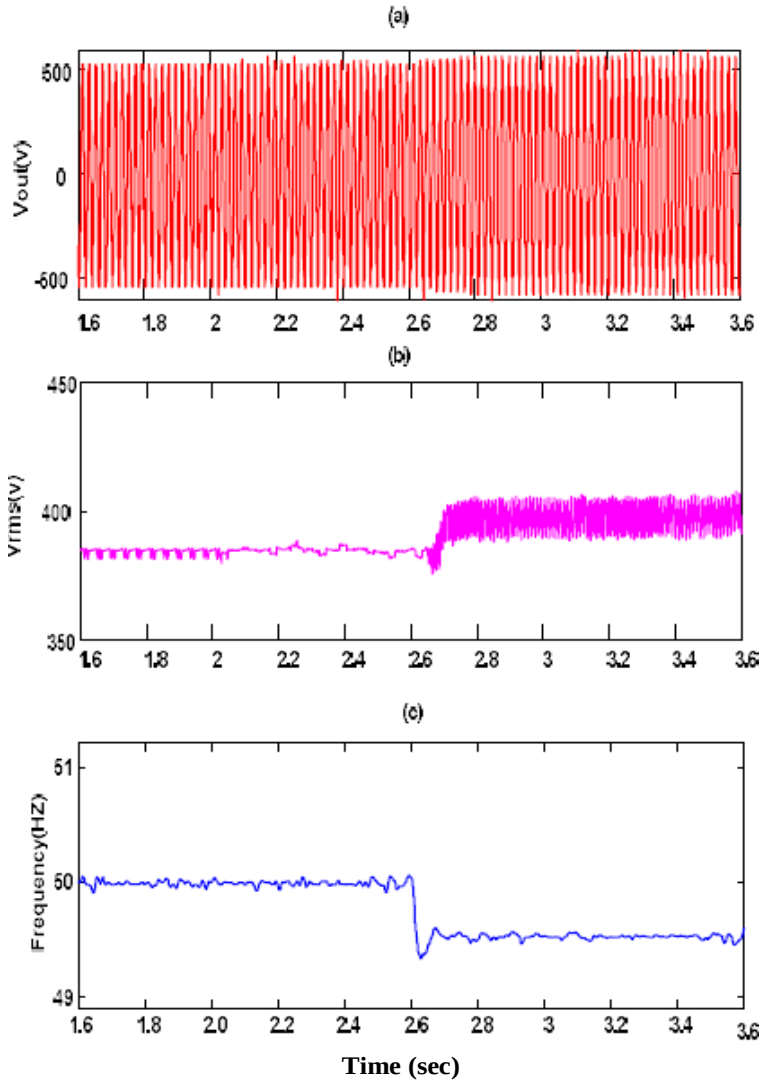

Figure 14. Mismatch power condition: (a) phase voltage, (b) RMS voltage value, (c) frequency.

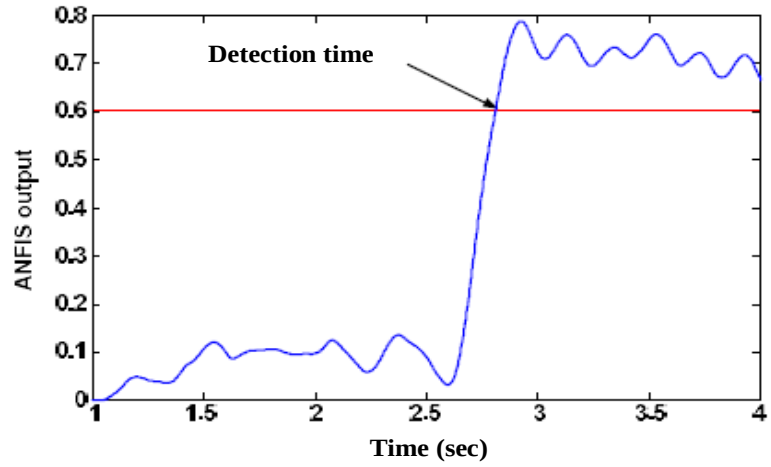

Figure 15. ANFIS output for mismatch power condition (2).

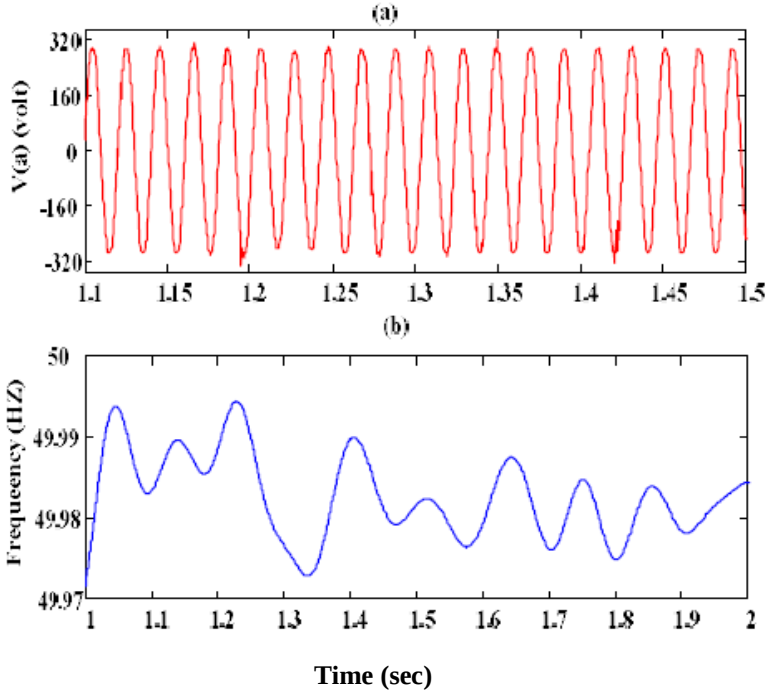

Figure 16. Motor starting condition: (a) three phase voltage, (b) frequency.

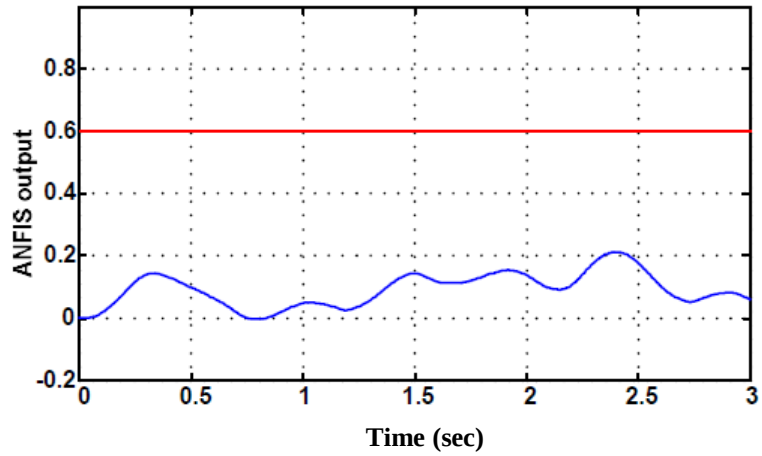

Figure 17. ANFIS output for motor starting.

algorithm produced the trip signal and sends to DG.

Motor starting condition

The starting of induction motors may cause a malfunction of the islanding detection algorithm. To study the reliability of the proposed algorithm, at t = 1.15 min an induction motor with P = 1KW and Q = 1.1 Kvar is starting and connected to the PCC. Figure 16a and b shows the waveforms of phase voltage and frequency of DGs, respectively. Figure 17 shows the ANFIS results at this condition. The value of neural network output is not reach to threshold value. Therefore, the proposed method does not send a trip signal to DG and works in a reliable mode.

Capacitor bank switching condition

Large capacitor bank switching in distribution power systems initiates disturbances. These disturbances are

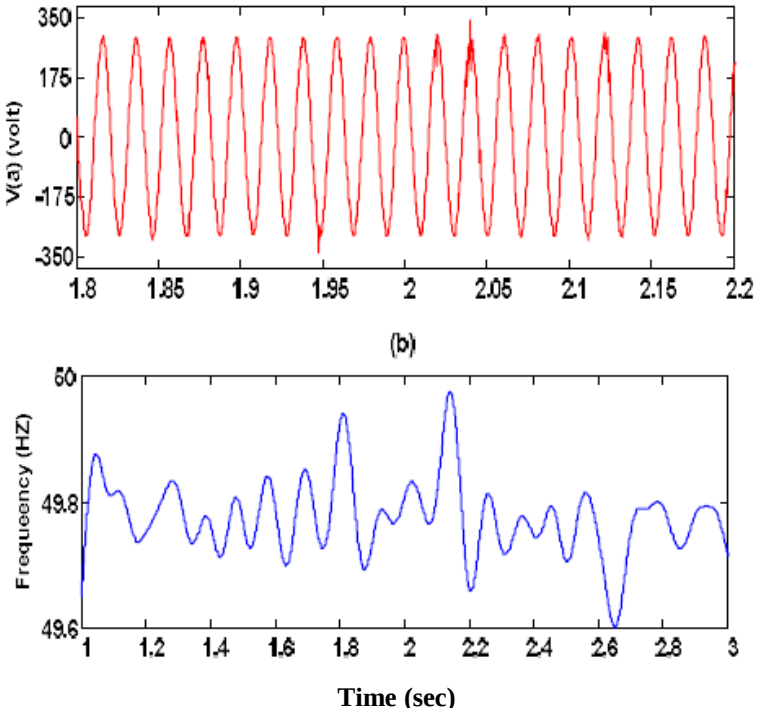

Figure 18. Capacitor bank switching condition: (a) three phase voltage, (b) frequency.

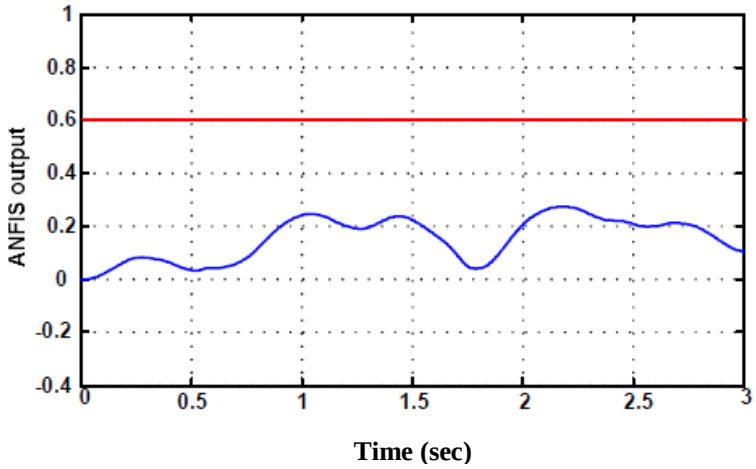

Figure 19. ANFIS output for motor starting.

propagated in the distribution system and have some effects on the proposed method. To test the proposed algorithm, at t = 2 s, a large 30 μF capacitor bank was switched at the PCC in the non-islanding case. In Figure 18a and b, the waveforms of phase voltage and frequency of DGs are individually depicted. Figure 19 shows the neural network response. The value of neural network output is not reach to threshold value too. Therefore, the system continue to working without any mistaken trip.

Conclusion

A new technique for islanding detection of DG is proposed based on ANFIS. Following the increased number and enlarged size of distributed generating units installed in a modern power system, the protection

against islanding has become extremely challenging nowadays. Islanding detection is also important as islanding operation of distributed system is seen a viable option in the future to improve the reliability and quality of the supply. The islanding situation needed to be prevented with DG due to safety reasons and to maintain quality of power supplied to the customers. By case studies with numerical simulations, the proposed approach was verified with feasibility, flexibility and robustness.

REFERENCES

Behrooz S, Hossein KK, Adel A (2011). A Mixed Active-Passive Algorithm for Islanding Detection of Wind Turbine DG Units. Int. Rev. Elect. Eng. 6(2):992-999.

Gupta MM, Rao DH (1994). Neuro-Control Systems: Theory and Applications. Piscataway, NJ: IEEE press.

Hernandez-Gonzalez G, Iravani R (2006). Current injection for active islanding detection of electronically-interfaced distributed resources. IEEE Trans. Power Deliv. 21(3):1698-705.

Hopewell PD, Jenkins N, Cross AD (1996). Loss-of-mains detection for small generators. IEE Proc – Elect Power Appl. 143(3):225-30.

http://www.renewableenergyworld.com/rea/news/article/2011/05/worldwind- outlook-down-but-not-out.

Hung GK, Chang CC, Chen CL (2003). Automatic phase-shift method for islanding detection of grid-connected photovoltaic inverters. IEEE Trans. Energy Convers. 18(1):169-173.

IEEE (2003). Standard for Interconnecting Distributed Resources into Electric Power Systems, IEEE Standard 1547TM, June 2003.

Imece AF, Jones RA, Sims TR, Gross CA (1989). An approach for modeling self commutated static power converters for photovoltaic islanding studies. IEEE Trans. Energy Convers. 4(3):397-401.

Jiayi H, Chuanwen J, Rong X (2008). A review on distributed energy resources and micro-grid. Renew. Sust. Energ Rev. 12:2472e83.

Karimi H, Yazdani A, Iravani R (2008). Negative-sequence current injection for fast islanding detection of a distributed resource unit. IEEE Trans. Power Elect. 23(1):298-307.

Smith GA, Onions PA, Infield DG (2000). Predicting islanding operation of grid connected PV inverters. IEEE Proc – Elect. Power Apply. 147(1):1-6.

Vachtsevanous G, Kang H (1989). Simulation studies of islanded behavior of grid connected photovoltaic systems. IEEE Trans. Energy Convers. 4(2):177-83.

Yen J, Langari R, Zadeh LA (1995). Industrial Applications of fuzzyLogic and Intelligent Systems. IEEE Press, New York, NY. P. 190.

Zeineldin HH, El-Saadany EF, Salama MMA (2006). Impact of DG interface control on islanding detection and non-detection zones. IEEE Trans. Power Deliv. 21(3):1515-23.

academicJournals

Vol. 8(27), pp. 1437-1441, 23 July, 2013
DOI: 10.5897/IJPS12.323
ISSN 1992-1950 © 2013 Academic Journals
http://www.academicjournals.org/IJPS

International Journal of Physical Sciences

Full Length Research Paper

Application of regression and multiple correlation analysis to morning hours solar radiation in Lapai

Agbo G. A.[1]*, Alfa B.[2], Ibeh G. F.[1] and Adamu I. S.[2]

[1]Department of Industrial Physics, Ebonyi State University, Abakaliki, Nigeria.
[2]Department of Physics, Ibrahim Badamasi Babangida University, Lapai, Nigeria.

Accepted 22 July, 2013

Solar radiation in Lapai within the morning hours has been estimated by correlating meteorological parameters. This was achieved by applying the first and second order regression and multiple correlation analysis method. The correlation coefficient based on the first and second order equations in temperature and relative humidity were 0.828, 0.692, 0.860 and 0.622 while the correlation coefficient based on the multiple correlations between solar radiations, temperature and relative humidity were 0.351. Validity tests were carried our using mean bias error (MBE), root mean square error (RMSE) and mean percentage error (MPE). The tests show that the errors were minimal in the first order equations in temperature and relative humidity. Comparison of the measured and predicted values of solar radiation based on the relative humidity and average temperature first order equations show a close agreement, and suggests the best equations to be used in estimating solar radiation in Lapai and its similar climatic condition.

Key words: Solar radiation, multiple regression, correlation coefficient, meteorological parameter-temperature, relative humidity.

INTRODUCTION

Solar radiation is the energy from the sun reaching the earth and is important in understanding the land atmosphere energy exchange (Liang et al., 2012). It is the driving force of both the physical and biological cycles on the earth. Consequently, it then becomes pertinent to have very good knowledge of current and past records of solar radiation at a location so as to aid in the estimation of the performance of any solar energy system. Pyrheliometer and pyranometer are instruments used readily to obtain the diffuse component of solar radiation and the global solar radiation, respectively. Meteorological stations have been used mostly for this purpose. However, there are a few of such stations across the globe and worse still in the developing countries. In order to develop solar radiation data, researchers had extrapolated values from one location for application in a different location. Hence, solar radiation prediction from estimation models has been widely utilized globally to generate solar radiation database for various location of the world. There are numerous statistical techniques of estimating solar radiation and each method is based on different principles. The first empirical correlation using sunshine hours for estimation of solar radiation was proposed by Angstrom (Ahmad and Ulfat, 2004). This model was later modified by Prescott and Page (Page, 1961; Ahmad and Ulfat, 2004; Maghrabi, 2009) in which the model is given as:

$$\frac{H}{H_o} = a + b\left(\frac{S}{S_o}\right),$$

*Corresponding author. E-mail: agbogodwina@yahoo.com.

Table 1. Climate parameters.

Parameter	Unit
Average temperature (T_{av})	°C
Relative humidity (R)	%
Solar radiation (H)	W/m^2

Where H is the monthly average daily global radiation on horizontal surface, H_o is the monthly average daily extra-terrestrial radiation, S is the length of the day, S_o is the maximum possible sunshine duration, and *a* and *b* are constants.

Since this development, there have been other models such as Rietveld, Bahel, Glover, Hay and Grag models (Mahdi et al., 1992). Akpabio et al. (2005) developed the quadratic form of Angstrom-Prescott model and used it to estimate the global solar radiation at Onne, Nigeria (latitude 4° 46′ N, Longitude 7° 10′ E). Multi-linear polynomial form of the Angstrom-Prescott model was employed by Agbo et al. (2010) to estimate global solar radiation at Minna, Nigeria. Various other models employing other meteorological parameters with one or more variables with solar radiation have also been used. The estimation of the solar radiation at Uturu in Nigeria was carried out using an equation relating solar radiation and temperature (Chiemeka, 2008). Agbo (2012) had also estimated 'global' solar radiation at Onitsha using regression

analysis and artificial neural network models with the attendant parameters of temperatures and relative humidity. Lapai is in Niger State of Nigeria and is located at latitude 9.05° N and longitude 6.05° E. The main stay of the economy in Lapai is agriculture and solar radiation is an important parameter for agriculture. However, the availability of such vital data is not readily available. Due to the present economic hardship in Nigeria, there is every tendency for having problems of maintaining and purchasing the instrument used in measuring the meteorological parameters in the meteorological stations.

The solution to this problem has motivated one into the need for an empirical modeling for estimation of solar radiation that will be affordable and easily maintained as it uses mathematical, statistical correlation and regression analysis for computation. The first time solar radiation was being measured in Lapai is in 2010 and even as that the measurements were not consistent due to instrument and power failure. Sometimes, when one wants to get the value of instant solar radiation to test the functioning of solar devices or to have idea or past records at any particular time so as to forecast crop yield for the next season, the instruments for measuring the solar radiation are not found or faulty. It is by this reason that this paper is written. Thus, the aim of this work is therefore to develop a relation between solar radiation with temperature or relative humidity or both for morning hours in Lapai. The morning hour records of 5 min intervals are the only record retrieved and made available by the recorder.

MATERIALS AND METHODS

The data (maximum and minimum temperatures, relative humidity and solar radiation) used in this study were obtained from the weather station located at Geography Department of Ibrahim Badamasi Babangida University, Lapai (IBBUL), Niger State, Nigeria. The data were collected at 5-min interval in the year 2010 and cover a time period of 9.30 to 10.30 am as there were inconsistency and missing data at early hours of the morning. The data were averaged over days that have meaningful records. The minimum and maximum temperatures were averaged to obtain the average temperature at each time interval. Table 1 shows the climatic parameters obtained with their units. In regression analysis, the first and second order regressions of normal equations were employed to estimate the morning hours global solar radiation as, thus, following the treatment in Agbo (2012); we have:

$$a + bx = y \quad (1)$$

$$a + bx + cx^2 = y \quad (2)$$

Where *a* and *b* are constants which will be determined. *y* is the same as solar radiation (H) and it is the dependent variable. *x* is the independent variable which can be replaced by any of the meteorological parameters such as average temperature and relative humidity.

To carry out the regression analysis of the first order, both sides of Equation 1 is multiplied by one and summed on both sides to yield Equation 3. Equation 1 also is multiplied by *x* and summed on both sides to yield Equation 4:

$$aN + b\Sigma x = \Sigma y \quad (3)$$

$$aN\Sigma x + b\Sigma x^2 = \Sigma xy \quad (4)$$

Applying the variables T_{av} and R for average temperatures and relative humidity respectively, as the independent variable in Equation 1 for first order regression we obtain:

$$a_1 N + b_1 T_{av} = H_1 \quad (5)$$

$$a_2 N + b_2 R = H_2 \quad (6)$$

To obtain the second order regression equation, Equation 2 is multiplied by 1, *x* and x^2 successively and summed to obtain the following equations:

$$a_1 N + b_2 \Sigma x + c_3 \Sigma x^2 = \Sigma y \quad (7)$$

$$a_1 N\Sigma x + b_2 \Sigma x^2 + c_3 \Sigma x^3 = \Sigma xy \quad (8)$$

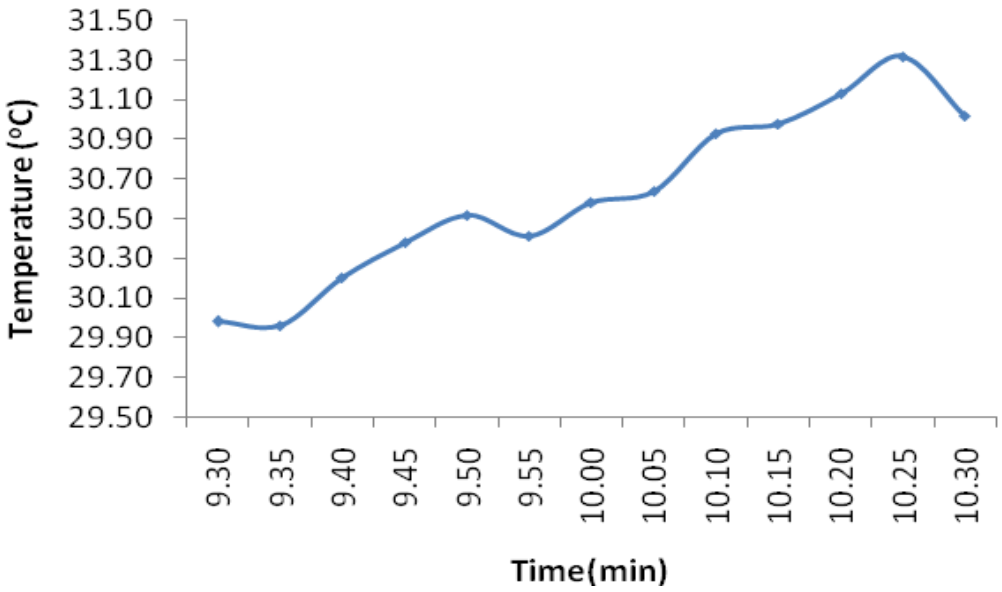

Figure 1. Variation of temperature with time in Lapia.

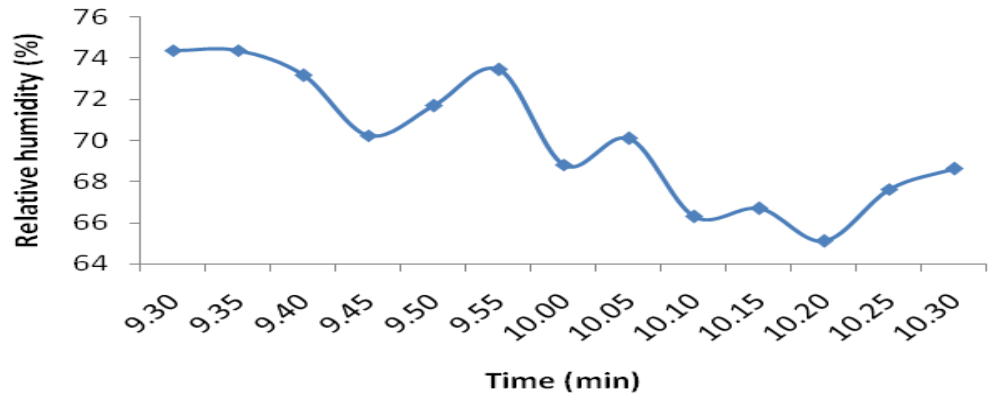

Figure 2. Relative humidity variation during the morning hours in Lapia.

$$a_1 N\Sigma x^2 + b_2\Sigma x^3 + c_3\Sigma x^4 = \Sigma x^2 y \quad (9)$$

Applying these equations by using our independent variables such as average temperature and relative humidity, we obtain:

$$a_3 + b_3 T_{av} + C_3 T_{av}^2 = H_3 \quad (10)$$

$$a_4 + b_4 R + C_4 R^2 = H_4 \quad (11)$$

RESULTS AND DISCUSSION

Figures 1 and 2 are the plots of the measured temperature and relative humidity as against time in Lapai. From the temperature plot (Figure 1), it shows that there is a continuous increase in temperature at early morning hours of the day while the relative humidity plot (Figure 2) shows a downward trend from early hours to before noon time hours. The trend variation as observed in temperature and relative humidity suggests that solar insolation at early morning hours in Lapai causes changes in the weather parameters. Figures 3 and 4 show the scatter plot of solar radiation against average temperature, and solar radiation against relative humidity, respectively. Despite the large amount of scattered points, definite correlations between them do exist. The large amount of scattered data is partly attributed to error in estimation of the solar radiation at 5-min intervals.

The first and second order regression equations obtained in this work using the average temperature and relative humidity are as follows:

$$H_1 = -2715.96 + 105.72 T_{av} \quad (12)$$

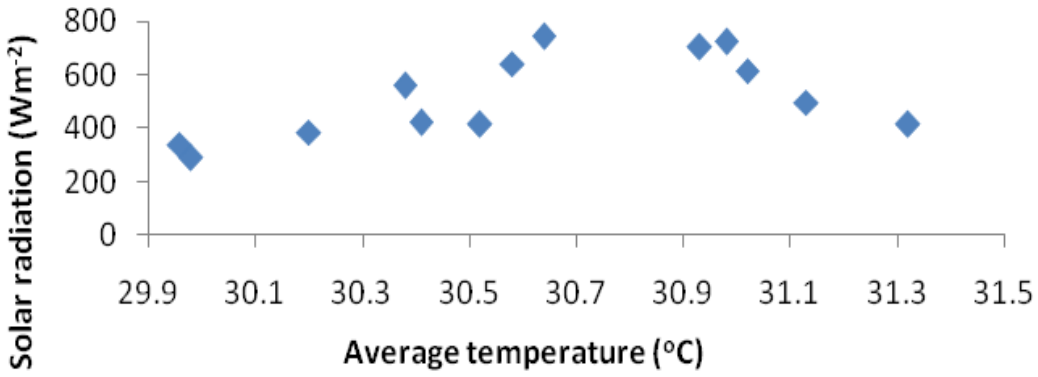

Figure 3. Scatter plot of solar radiation against average temperature.

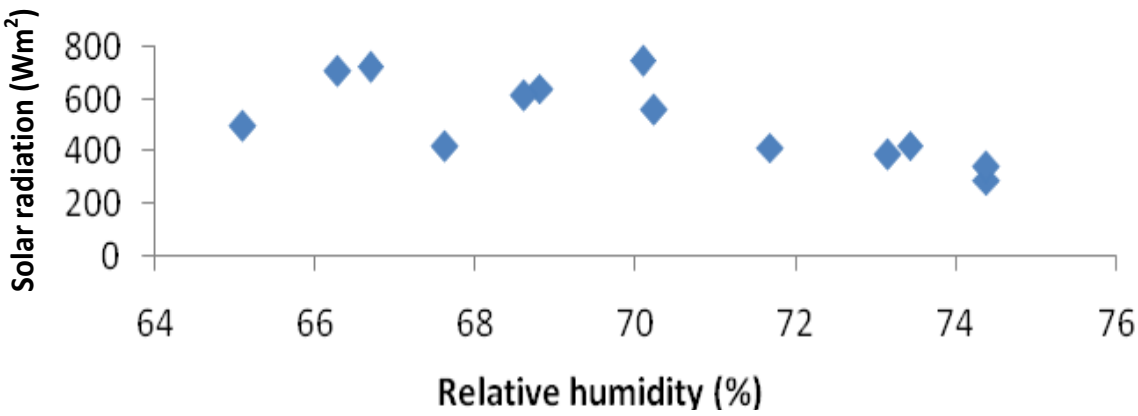

Figure 4. Scatter plot of solar radiation against relative humidity.

$$H_2 = 2883.77 - 33.094R \quad (13)$$

$$H_3 = -5011.04 + 175.08T_{av} + 0.81T_{av}^2 \quad (14)$$

$$H_4 = 698.60 - 1.70R - 0.012R^2 \quad (15)$$

The multiple regression equation of solar radiation with average temperature and relative humidity were obtained as:

$$H_5 = -20.89R + 64.77T_{av} \quad (16)$$

The correlation based on the average temperature alone is obtained as 0.828 and relative humidity alone is 0.860. The estimated results from each of the average temperature and relative humidity show a closer agreement to the measured data than that predicted from the correlation based on the average temperature and relative humidity taken together. A comparison of the result of Equation 12, 13, 14, 15 and 16 indicates that the correlation of Equation 13 based on the relative humidity alone and Equation 12 based on average temperature alone should be employed for computing solar radiation in the morning hours in Lapai. The deviations between the measured and estimated values of the solar radiation have been evaluated. This is in an effort to test the validity of the equations for the solar radiation. As seen from Table 2, the percentage errors are very small and the equations may be taken as valid equations for estimating solar radiation in the morning hours in Lapai. The validity of the equations were also tested using mean bias error (MBE), root mean square error (RMSE) and correlation coefficient (CC) which gave good results as seen in Table 2.

Figure 5 shows the relationship between the measured solar radiation and the estimated solar radiation using each of the equations as aforementioned.

Conclusion

In this study, an attempt has been made at estimating solar radiation based on meteorological data at IBBUL.

Table 2. Summary of calculations.

Equations	CC	CD	MBE	RMSE	MPE
$H_1 = -2715.96 + 105.72T_{av}$	0.828	0.686	-0.189	0.682	0.003
$H_2 = 2883.77 – 33.094R$	0.860	0.740	0.004	0.016	-0.001
$H_3 = -5011.04 + 175.08T_{av} + 0.81T_{av}^2$	0.692	0.479	0.419	1.152	-0.006
$H_4 = 698.60 – 1.70R – 0.012R^2$	0.622	0.387	-0.217	0.782	0.003
$H_5 = -20.89R + 64.77T_{av}$	0.351	0.123	0.538	1.939	0.008

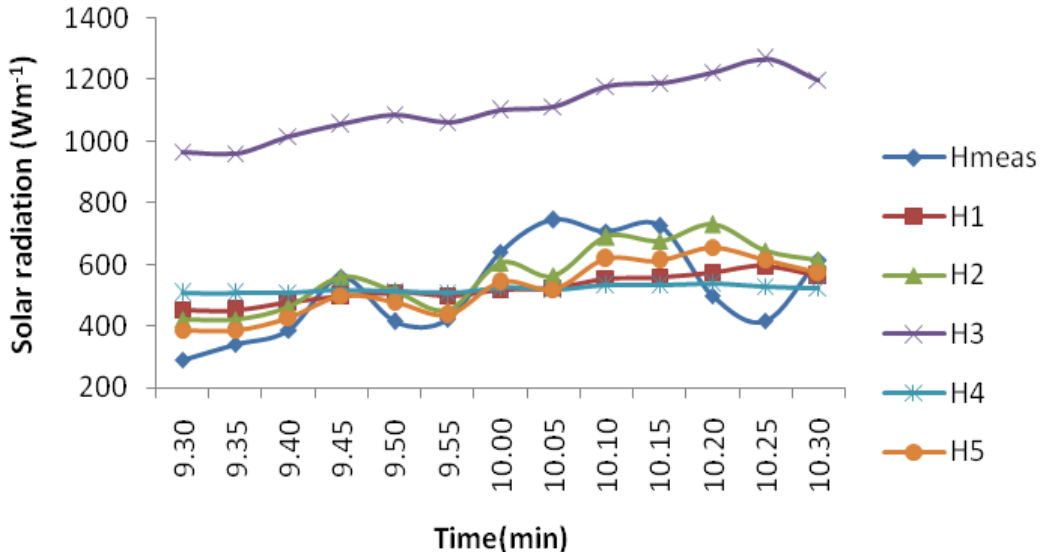

Figure 5. Measured and estimated values of solar radiation.

The results of the estimated values show a closer agreement to the measured data. The results were obtained using first and second order regression and multiple regression analysis which portrays a good correlation. The deviations between the measured and estimated values were minimal. The results from this analysis will greatly reduce the problem associated with waste of time and lack of efficient instruments. It will also be an easy way to present data and ensure that data never runs out. This will also allow user of the data to track information of solar radiation data in Lapai.

ACKNOWLEDGEMENT

The authors are grateful to the Geography Department of the IBBUL for making the data obtained from the automatic weather station available. The first author thanks the vice-Chancellor of IBBUL for granting him the honour of spending one-year sabbatical leave with the Physics Department of the University. Thanks to Mr. Samuel in the Geography Department of the University.

REFERENCES

Agbo GA, Baba A, Obiekezie TN (2010). Empirical Models for the correlation of monthly average global solar radiation with sunshine hour at Minna, Nig. J. B. Res. 1 (1):41-47.

Agbo GA (2012). Estimation of Global Solar Radiation at Onitsha with Regression analysis and artificial Neural Network Models. Res. J. Recent. Sci. 1 6):1-8.

Ahmad F, Ulfat I (2004). Empirical Models for the correlation of monthly average daily global solar radiation with hours of sunshine on a horizontal surface at Karachi, Pakistan. Turk. J. Phys. 28:301-307.

Akpabio LE, Udo SO, Etuk SE (2005). Modeling Global Solar Radiation for a Tropical Location: Onne, Nigeria. Turk. J. Phys. 29:63-68.

Chiemeka IU (2008). Estimation of solar radiation at Uturu, Nigeria. Inter. J. Phys. Sci. 3 (5):126-130.

Liang H, Zhang R, Liu J, Sun Z, Cheng X (2012). Estimation of Hourly Solar Radiation at the Surface under Cloudless Conditions on the Tibetan Plateau Using a Simple Radiation Model Adv.Atm.Sci. 29(4):675-689.

Maghrabi AN (2009). Parameterization of a simple model to estimate monthly global solar radiation bases on meteorological variables and evaluation of existing solar radiation models for Tabouk, Saudi Arabia. Energy conversion and management. 50:2754 –2760.

Mahdi NL, Baharn NS, Zaki FF (1992). Assessment of solar radiation models for the Gulf Arabian countries. Renew. Energy 2(1):65-71.

Page JK (1961). The estimation of monthly mean values of daily total shortwave radiation on vertical and inclined surfaces from sunshine records for latitudes 40°N – 40°S. In proceedings of UN conference on new sources of energy. pp. 378-390.

UPCOMING CONFERENCES

ICNMB 2013 : International Conference on Nuclear Medicine and Biology Switzerland, Zurich, July 30-31, 2013

International Conference on Mathematical Modeling in Physical Sciences Prague, Czech Republic, September 1-5, 2013

Conferences and Advert

July 2013
ICNMB 2013 : International Conference on Nuclear Medicine and Biology
Switzerland, Zurich, July 30-31, 2013

September 2013
International Conference on Mathematical Modeling in Physical Sciences
Prague, Czech Republic, September 1-5, 2013

International Journal of Physical Sciences

Related Journals Published by Academic Journals

- *African Journal of Pure and Applied Chemistry*
- *Journal of Internet and Information Systems*
- *Journal of Geology and Mining Research*
- *Journal of Oceanography and Marine Science*
- *Journal of Environmental Chemistry and Ecotoxicology*
- *Journal of Petroleum Technology and Alternative Fuels*

academicJournals